

ARTICLE OPEN



Circadian rhythm disruptions associated with opioid use disorder in synaptic proteomes of human dorsolateral prefrontal cortex and nucleus accumbens

Stephanie Puig^{1,2}, Xiangning Xue³, Ryan Salisbury², Micah A. Shelton², Sam-Moon Kim², Mariah A. Hildebrand^{1,2}, Jill R. Glausier^{1,2}, Zachary Freyberg^{1,2,4}, George C. Tseng³, Anastasia K. Yocum⁵, David A. Lewis^{1,2}, Marianne L. Seney^{1,2}, Matthew L. MacDonald^{2,6} and Ryan W. Logan^{1,2,6,7}✉

© The Author(s) 2023

Opioid craving and relapse vulnerability is associated with severe and persistent sleep and circadian rhythm disruptions. Understanding the neurobiological underpinnings of circadian rhythms and opioid use disorder (OUD) may prove valuable for developing new treatments for opioid addiction. Previous work indicated molecular rhythm disruptions in the human brain associated with OUD, highlighting synaptic alterations in the dorsolateral prefrontal cortex (DLPFC) and nucleus accumbens (NAc)—key brain regions involved in cognition and reward, and heavily implicated in the pathophysiology of OUD. To provide further insights into the synaptic alterations in OUD, we used mass-spectrometry based proteomics to deeply profile protein expression alterations in bulk tissue and synaptosome preparations from DLPFC and NAc of unaffected and OUD subjects. We identified 55 differentially expressed (DE) proteins in DLPFC homogenates, and 44 DE proteins in NAc homogenates, between unaffected and OUD subjects. In synaptosomes, we identified 161 and 56 DE proteins in DLPFC and NAc, respectively, of OUD subjects. By comparing homogenate and synaptosome protein expression, we identified proteins enriched specifically in synapses that were significantly altered in both DLPFC and NAc of OUD subjects. Across brain regions, synaptic protein alterations in OUD subjects were primarily identified in glutamate, GABA, and circadian rhythm signaling. Using time-of-death (TOD) analyses, where the TOD of each subject is used as a time-point across a 24-h cycle, we were able to map circadian-related changes associated with OUD in synaptic proteomes associated with vesicle-mediated transport and membrane trafficking in the NAc and platelet-derived growth factor receptor beta signaling in DLPFC. Collectively, our findings lend further support for molecular rhythm disruptions in synaptic signaling in the human brain as a key factor in opioid addiction.

Molecular Psychiatry (2023) 28:4777–4792; <https://doi.org/10.1038/s41380-023-02241-6>

INTRODUCTION

Rates of opioid use disorder (OUD) and deaths from opioid overdoses have continued to rise in the United States over the recent decade (2012–2022) [1]. Further understanding of the impact of long-term opioid use and opioid overdose on the human brain is important for considering new avenues of treatment and intervention. Investigating the molecular alterations in postmortem brains from subjects with OUD provide valuable insights into the neurobiological mechanisms and potential therapeutic targets for opioid addiction [2–8].

Recent work in postmortem brains of subjects with OUD from us [2, 3] and others [4, 6, 9, 10] have primarily focused on the dorsolateral prefrontal cortex (DLPFC) and nucleus accumbens (NAc), key brain regions involved in cognition and reward, which are significantly impacted in OUD [11–13]. An interplay between inflammation and synaptic remodeling associated with OUD in both DLPFC and NAc has been a consistent finding across human

postmortem brain studies [3, 9, 10]. Most recently, our work linked alterations in neuroinflammatory, dopaminergic, and GABAergic signaling in DLPFC and NAc of OUD subjects with significant disruptions in circadian rhythms of transcript expression [2]. In OUD, alterations in transcriptional rhythms were associated with sleep and circadian traits (e.g., insomnia) [2], further supporting biological relationships between changes in sleep, circadian rhythms, and synaptic signaling in opioid addiction [14–22].

To date, much of the work has used transcriptomics approaches to investigate the molecular alterations in postmortem brains of subjects with OUD, with limited studies using proteomics [10]. Complementary to transcriptomics, proteomics can report on functionally relevant information in cell bodies and neuropils, including synapses and glial processes [23–25]. Recent advances have enabled reliable detection of numerous peptides in synaptosomes isolated from postmortem human brains [24]. Deep profiling of protein changes at the synaptic level may lead to

¹Department of Pharmacology, Physiology and Biophysics, Boston University School of Medicine, Boston, MA, USA. ²Department of Psychiatry, University of Pittsburgh School of Medicine, Pittsburgh, PA, USA. ³Department of Biostatistics, University of Pittsburgh, Pittsburgh, PA, USA. ⁴Department of Cell Biology, University of Pittsburgh, Pittsburgh, PA, USA. ⁵AZIDEA, LLC, Ann Arbor, MI, USA. ⁶Department of Psychiatry, University of Massachusetts Chan Medical School, Worcester, MA, USA. ⁷Department of Neurobiology, University of Massachusetts Chan Medical School, Worcester, MA, USA. ✉email: macdonaldml@upmc.edu; ryan.logan@umassmed.edu

Received: 10 April 2023 Revised: 18 August 2023 Accepted: 25 August 2023

Published online: 6 September 2023

functional insights into disease-related mechanisms associated with psychiatric disorders.

Using quantitative mass spectrometry (MS) and tandem mass tags (TMT) [26, 27], we profiled both tissue homogenates and synaptosomes isolated from postmortem DLPFC and NAc of unaffected subjects to compare tissue- and synapse-level protein expression to subjects with OUD. Our approach allowed us to identify proteins that were preferentially expressed, or enriched, specifically in synapses of DLPFC and NAc, and assess synapse-specific alterations associated with OUD. Overall, pathways related to neuroinflammation, and neurodegeneration were altered across brain regions in OUD, accompanied by significant changes in proteins involved in GABAergic and glutamatergic synaptic signaling. Notably, synaptic alterations associated with OUD occurred in parallel to disruptions in pathways of circadian rhythm regulation. To further explore circadian rhythms in human postmortem brain, we used time-of-death (TOD) analysis to capture alterations associated with OUD in the diurnal variation of protein expression in synaptosomes. In synapses, disruptions to molecular rhythms were primarily related to endoplasmic reticulum functions, including protein trafficking and vesicle-mediated transport, platelet-derived growth factor receptor (PDGFR) signaling, and proteins involved in GABA and glutamate synaptic signaling. Collectively, our results suggest protein pathways related to neurodegeneration are altered at the tissue level in DLPFC and NAc of OUD subjects, with implications for opioid-induced changes in circadian regulation of inhibitory and excitatory synaptic signaling.

MATERIALS AND METHODS

Human subjects

Following consent from next-of-kin, postmortem brains were obtained during autopsies at Allegheny County (Pittsburgh, PA, USA; $N=39$) or Davidson County (Nashville, TN, USA; $N=1$) Medical Examiner's Office. An independent committee of clinicians made consensus, lifetime DSM-IV diagnoses for each subject based on results from psychological autopsy, including structured family interviews, medical record reviews, and toxicological and neuropathological reports [28]. Similar procedures were used to confirm absence of lifetime psychiatric and neurological disorders in unaffected subjects. Procedures were approved by University of Pittsburgh Committee for Oversight of Research and Clinical Training Involving Decedents and Institutional Review Board for Biomedical Research. Cause of death in 19/20 OUD subjects was accidental, due to combined drug or opioid overdose. Accordingly, toxicology revealed that 19/20 OUD subjects had detectable opioids in their blood at time of death (Supplementary Table 1). Each OUD subject was matched with an unaffected comparison subject for sex, age, and postmortem interval (PMI) [2, 3]. Cause of death for unaffected subjects was either natural, accidental, or undetermined (Supplementary Table 1; opioids absent by blood toxicology). Cohorts differed by race ($p=0.02$) and brain pH ($p=0.015$, 0.2 pH units mean difference), and did not significantly differ in PMI, RNA integrity number (RIN), or TOD ($p > 0.25$; Supplementary Table S1). TOD was determined from the death investigation report (Medical Examiner's Office). DLPFC (Brodman Area 9) and NAc were anatomically identified and collected, as previously described [2, 3].

Brain sample preparation for mass spectrometry

Gray matter tissue (~20 mg) from DLPFC and NAc were collected from fresh-frozen coronal tissue blocks via cryostat to minimize contamination from white matter and other subregions [29, 30]. Homogenate and synaptosome preparations were obtained using a variation of our enrichment protocol for postmortem human brain tissues [24, 31, 32] with SynPER reagent (ThermoFisher). From each sample, 10 μ g total protein (as measured by Micro BCA) was reduced, alkylated, and trypsin digested on S-Trap™ micro spin columns (ProtiFi). Subject pairs were randomly assigned to TMT blocks and labeled with TMTPro channels 1–10, with brain regions and preparations assigned to separate blocks [33]. Additional aliquots from each sample were used for a pooled control, digested separately with S-Trap Midi™ columns, divided then labeled with TMTPro channels 1 and 12. TMT labeled preparations from the same block were pooled with 10 μ g of the labeled pooled controls. The TMT labeled

peptide pools were separated into eight fractions with the Pierce™ High pH Reversed-Phase Peptide Fractionation Kit (ThermoFisher Scientific), evaporated, and reconstituted in 20 μ l 97% H₂O, 3% ACN, 0.1% formic acid.

Mass spectrometry

TMT labeled peptides (~1 μ g) were loaded onto a heated PepMap RSLC C18 column (2 μ m, 100 Å, 75 μ m \times 50 cm; ThermoScientific), then eluted by gradients optimized for each high pH reverse-phase fraction [27]. Sample eluate was electrosprayed (2000 V) into an Orbitrap Eclipse Mass Spectrometer (MS; ThermoFisher Scientific) for analysis. MS1 spectra were acquired at a resolving power of 120,000. MS2 spectra were acquired in the Ion Trap with CID (35%) in centroid mode. Real-time search (RTS) (max search time = 34 s; max missed cleavages = 1; Xcorr = 1; dCn = 0.1; ppm = 5) was used to select ions for SPS for MS3. MS3 spectra were acquired in the Orbitrap with HCD (60%) with an isolation window = 0.7 m/z and a resolving power of 60,000, and a max injection time of 400 ms.

Data processing

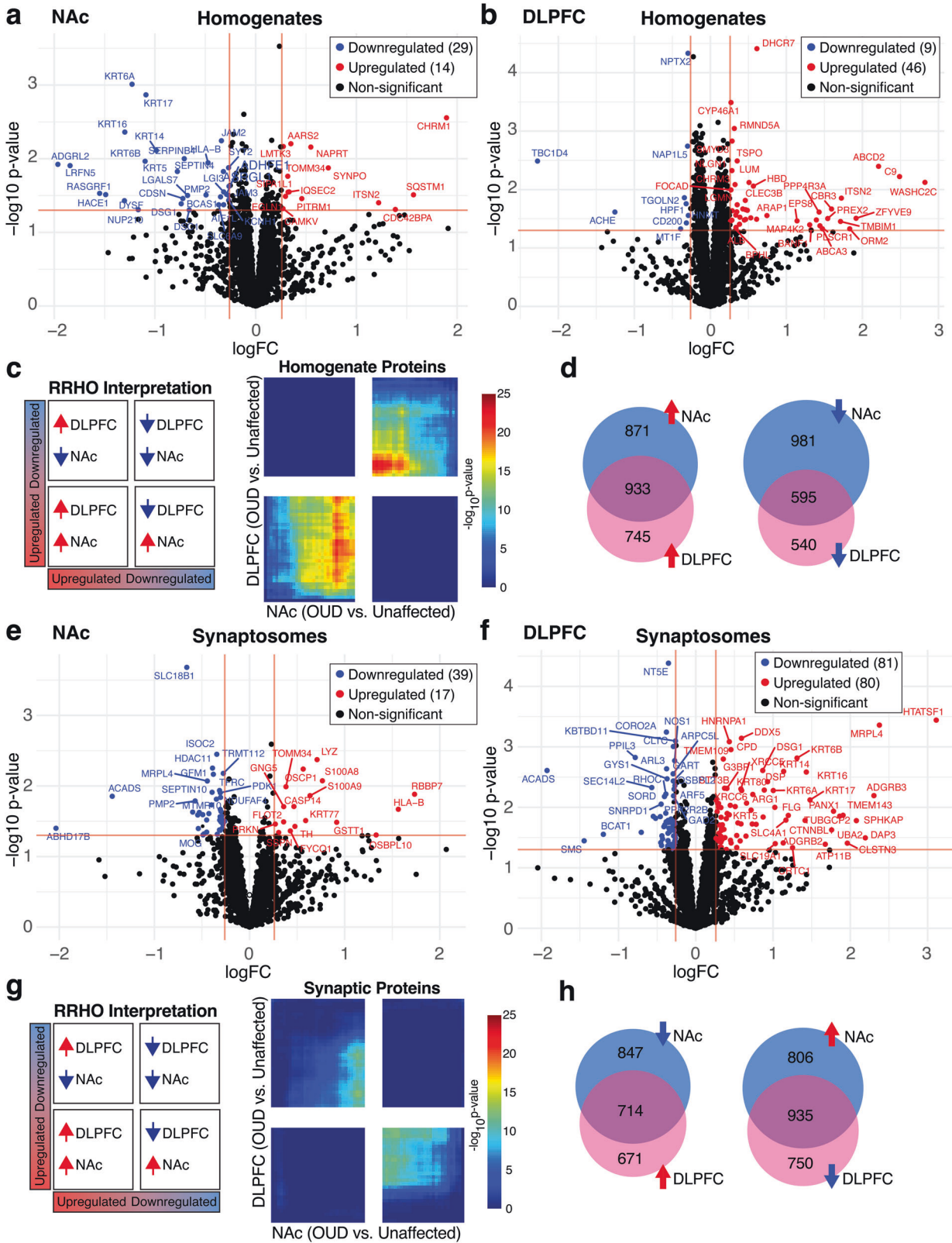
Raw MS files were processed in Proteome Discoverer (v. 2.5; ThermoFisher Scientific). MS spectra were searched against the *Homo sapiens* SwissProt database. SEQUEST search engine was used (enzyme=trypsin, maximum missed cleavage=2, minimum peptide length=6, precursor tolerance=10ppm). Static modifications include acetylation (N-term, +42.011 Da), Met-loss (N-term, -131.040 Da), Met-loss+Acetyl (N-term, -89.030 Da), and TMT labeling (N-term and K, +229.163 Da). Dynamic modification, oxidation (M, +15.995 Da). PSMs were filtered by the Percolator node (maximum Delta Cn=0.05, FDR=0.01). Reporter ion quantification was based on intensity values with the following settings/filters: integration tolerance=20ppm, method=most confident centroid, co-isolation threshold = 100, and SPS mass matches [%] threshold = 65. Peptide intensity values were normalized within and across TMT plex runs with Normalization Mode = Total Peptide Amount and Scaling Mode = On All Average in Proteome Discoverer. Peptides used to sum to protein measures were determined using "Unique + Razor". Only proteins of high confidence were retained for analyses and protein values were log₂ transformed prior to analysis. The mass spectrometry proteomics data have been deposited to the ProteomeXchange Consortium via the PRIDE partner repository [34] with the dataset identifier PXD041333 and 10.6019/PXD041333.

Differential expression of proteins

Limma-Voom with covariate selection (TMT plex, sex, age, PMI, and peptide expression) was used to detect differentially expressed (DE) proteins between OUD and unaffected subjects in homogenate and synaptosome fractions [24]. Proteins were considered DE if both $p \leq 0.05$ (unadjusted) and log₂ fold-change (logFC) were greater than or equal to ± 0.26 (20% change in expression), as previously used [3, 35, 36]. Over-representation pathway analyses were completed using clusterProfiler [37] and ReactomePA [38] for DE proteins. Rank-rank hypergeometric overlap (RRHO) was used to detect overlap of proteins expression changes between unaffected and OUD subjects. To assess preferential enrichment of proteins in synapses, we compared protein expression between homogenate and synaptosomes within unaffected subjects and separately, within OUD subjects. Protein abundance in synaptosomes was compared to abundance in homogenates to identify proteins with significantly greater levels of expression in synaptosomes (Bonferroni-corrected $p < 0.05$). Proteins that showed a difference of at least 1.25-fold in the synaptosome relative to homogenates were classified as synapse-enriched proteins. All other proteins, by default, were defined as non-enriched. Analysis of synaptosome differences between unaffected and OUD subjects were limited to these enriched synaptic proteins, as described previously [24].

Diurnal rhythmicity analysis

For each subject, TOD was converted to Zeitgeber Time (ZT) by using the times of sunrise and sunset on the day of death (ZT0 is sunrise, negative ZTs reflect hours prior to sunrise). Sinusoidal curves were fitted using nonlinear least-squares regression with the coefficient of determination used as a proxy of goodness-of-fit (R^2). Estimates of empirical p -values were determined using null distributions of R^2 generated from 1000 TOD-randomized expression datasets. Diurnal rhythms of protein expression in homogenates and synaptosomes were identified separately in unaffected and OUD subjects. Rhythmic proteins were then compared between unaffected and OUD subjects ($p < 0.05$; Fisher's exact test). A complementary analysis determined which proteins exhibited a significant change in



rhythmicity between unaffected and OUD subjects ($\Delta R^2 = R^2 \text{ Unaffected} - R^2 \text{ OUD}$). Change in rhythmicity analysis was restricted to proteins that were significantly rhythmic in unaffected or OUD subjects. Proteins were identified as significantly less rhythmic in OUD versus unaffected subjects if $\Delta R^2 > 0$ or more rhythmic if $\Delta R^2 < 0$. Null distributions of ΔR^2 were permuted 1000 times, whereby the unaffected and OUD subjects were permuted

independently to generate null distributions (R^2 unaffected and R^2 OUD). Significantly less or more rhythmic in OUD was calculated by comparing the ΔR^2 to the null ΔR^2 for unaffected and OUD subjects. Differences in phase, amplitude, and base (mesor of fitted curve) were also calculated and restricted to significantly rhythmic proteins from both unaffected and OUD subjects. Pathway enrichments of rhythmic proteins were

Fig. 1 Proteomic alterations in tissue homogenates from NAc and DLPCF in subjects with OUD. **a** Log₂FC plotted relative to $-\log_{10} p$ value by volcano plot for DE proteins in NAc homogenates. **b** Log₂FC plotted relative to $-\log_{10} p$ value by volcano plot for DE proteins in DLPCF homogenates. **c** RRHO plot indicating weak overlap or concordance of protein alterations between DLPCF and NAc in OUD subjects. **d** Venn diagrams of downregulated and upregulated proteins between NAc and DLPCF homogenates. **e** Log₂FC plotted relative to $-\log_{10} p$ value by volcano plot for DE proteins in NAc synaptosomes. **f** Log₂FC plotted relative to $-\log_{10} p$ value by volcano plot for DE proteins in DLPCF synaptosomes. **g** RRHO plot indicating very weak discordance of protein expression alterations in OUD between DLPCF and NAc synaptosomes. **h** Venn diagrams of downregulated and upregulated proteins between NAc and DLPCF synaptosomes. Horizontal red lines indicate significance cutoffs of $p < 0.05$, with vertical red lines represent $\log_2 FC \pm 0.26$ (**a**, **b**, **e**, and **f**). Proteins that reached both unadjusted $p < 0.05$ and $\log_2 FC \pm 0.26$ were identified as DE proteins, upregulated labeled as red circles and downregulated labeled as blue circles.

completed by Metascape (Gene Ontology; Hallmark; Reactome; Canonical; metascape.org) [39].

Heatmaps represent the top rhythmic proteins in homogenates and synaptosomes for each brain region, whereby each row represents a protein, and each column represents a subject, ordered by ZT. Protein expression was Z-transformed and ordered by phase (ZT of peak expression). Heatmaps were generated for: (1) top 200 rhythmic proteins in unaffected subjects; (2) top 200 rhythmic proteins identified in unaffected subjects then plotted for OUD subjects to assess circadian proteomic alterations in OUD; (3) top rhythmic proteins in OUD subjects; (4) top 200 rhythmic proteins in OUD subjects then plotted for unaffected subjects.

Weighted gene co-expression network analysis

To identify co-expression protein modules, we used weighted gene co-expression network analysis (WGCNA) on protein expression from homogenates or synaptosomes within each brain region and group [2, 3, 40–42]. Module differential connectivity (MDC) analyses examined the impact of OUD on protein co-expression network modules. For each module, the degree of connection was calculated in both unaffected and OUD subjects. MDC was defined as the ratio of the protein co-expression connections between unaffected and OUD subjects. To assess significance of MDC, we permuted (1000 times) the samples and module members to generate null distribution. When a module was built on unaffected subjects, a significant MDC greater than 1 indicated a gain of connectivity of the modules in OUD, while a significant MDC less than 1 indicated a loss of connectivity. Modules were tested for enrichment of DE proteins and rhythmic proteins in unaffected and OUD. ARACNe was used to identify hub proteins in each module [43]. Proteins with an adjacency value higher than the 90th quantile were considered neighbors. Hub proteins were identified with the highest number of N-hub neighborhood nodes (NHNN) than the average. Hub proteins specific to unaffected and OUD subjects were considered disease-specific hub proteins. Hub gene networks were plotted using Cytoscape (3.9.1). We then identified enriched pathways of synapse-specific protein co-expression networks using SynGo [44].

RESULTS

Brain region-specific protein alterations in tissue homogenates and synaptosomes associated with OUD in NAc and DLPCF

Between unaffected and OUD subjects, we investigated protein expression differences in tissue homogenates of DLPCF and NAc and isolated synaptosomes from each brain region. We identified 43 DE ($p < 0.05$ and $\log_2 FC \pm 0.26$) proteins (14 upregulated and 29 downregulated; Fig. 1a, Supplementary Tables S2 and S3) in the NAc of subjects with OUD. In DLPCF, we identified 55 DE proteins, with most being upregulated in OUD (46 upregulated and 9 downregulated; Fig. 1b, Supplementary Tables S4 and S5). In synaptosomes, we found 56 DE proteins (17 upregulated and 39 downregulated) in NAc (Fig. 1e, Supplementary Tables S7, S8) and 161 DE proteins (80 upregulated and 81 downregulated) in DLPCF (Fig. 1f, Supplementary Tables S9 and S10).

To investigate the possible overlap of protein changes between brain regions, we compared protein expression between NAc and DLPCF of OUD subjects using the threshold-free approach, RRHO [45]. Overall, there was weak concordance of proteins that were upregulated or downregulated between brain regions of OUD subjects (Fig. 1c), despite identifying overlapping proteins between these brain regions (Fig. 1d). In contrast, we previously

reported remarkable concordance between NAc and DLPCF in both upregulated and downregulated transcripts associated with OUD of the same subjects investigated here [2, 3]. In synaptosomes, we identified no significant overlap of protein changes between brain regions (Fig. 1g, h). Therefore, protein alterations in OUD were unique within brain region, and together with our previous results [3], may reflect the impact of opioids and other factors on brain region-specific, post-transcriptional and translational processing.

Alterations in inflammatory and neurodegeneration-related pathways associated with OUD in NAc and DLPCF homogenates

To further define the biological significance of protein changes in OUD, we conducted pathway enrichment analysis on DE proteins from tissue homogenates of NAc and DLPCF (Fig. 2, Supplementary Table S6). In NAc homogenates, enrichment analyses identified pathways related to immune modulatory pathways, including various types of infection (e.g., KRT14,16,17 [46]; HLA-B [47]) and leukocyte migration (e.g., JAM2 [48]; PLCG1 [49]). Neurodegeneration-related pathways were also enriched in NAc homogenates (Fig. 2a; e.g., CHRM1 [50, 51]; MAPT [52]; SQSTM1 [53]). Similarly, several pathways related to neurodegeneration were highly enriched in DLPCF homogenates from OUD subjects, such as Alzheimer (43 proteins; e.g., SLC25A6 [54]; CHRM3 [55]; MTOR [56]; ITPR2 [57]), Huntington (38 proteins; e.g., PSM11 [58]; ADRM1 [59]; SOD1 [60]), Parkinson (41 proteins; PARK7 [61]; HTRA2 [62]), and prion (42 proteins; e.g., RYR2 [63]) disease-related pathways (Fig. 2b). Other pathways enriched in DLPCF homogenates were related to cell stress including oxidative phosphorylation and reactive oxygen species (Fig. 2b). Together, our findings highlight a possible cascade of immune activation, diminished cellular health, and initiation of neurodegenerative processes in human brain that are associated with OUD.

Differential enrichment between tissue homogenates and synaptosomes highlights altered GABAergic and glutamatergic synaptic signaling in NAc and DLPCF associated with OUD

We investigated protein expression changes preferentially enriched in synaptosomes to identify synapse-specific proteome alterations associated with OUD. We identified proteins primarily expressed in homogenates and preferentially expressed in synaptosomes within each brain region (Supplementary Tables S7–S12). Synapse-enriched proteins were then used for DE and pathway analyses comparing unaffected and OUD subjects. Synaptosomes isolated from NAc were enriched for several pathways involved in mitochondrial and endoplasmic reticulum functions (proximal tubule bicarbonate reclamation, carbohydrate digestion and absorption), along with second messenger signaling cascades (cGMP-PKG and cAMP: e.g., GNAI2,3; GABRA2; ACY1; Fig. 2a, Supplementary Table S6). Other pathways were specifically enriched in DLPCF synaptosomes from OUD subjects, which included ribosome, relaxin, and Rap1 signaling (Fig. 2b). OUD-associated alterations in serotonergic synapses (e.g., GNAO1; GNAS; GNAI2,3, GNB1,4) were also unique to DLPCF (Fig. 2b, Supplementary Table S2).

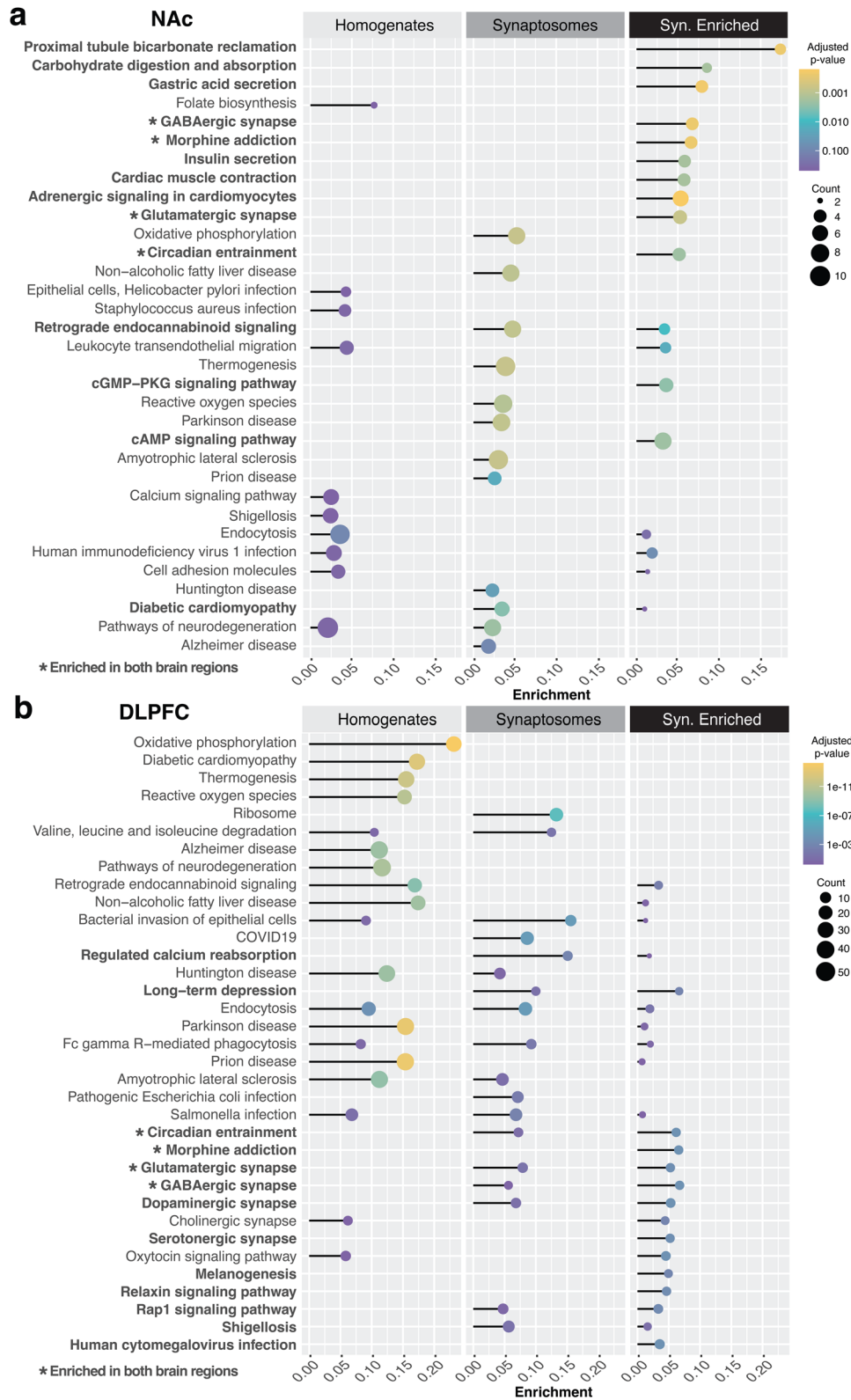


Fig. 2 Differential enrichment of synaptic proteins between NAC and DLPFC associated with OUD. Lollipop plot showing pathways enriched from DE proteins in synaptosomes relative to homogenates in **a** NAC and **b** DLPFC. Adjusted p value by color. Size of the circle represents counts of proteins within pathways. The enrichment score is calculated as the count of proteins identified as DE in OUD subjects divided by the count of proteins in the background of the respective ontological pathway. Bolded text with stars represents pathways enriched in both brain regions. Bolded only text represents pathways enriched in synaptosomes of the region analyzed. Also see Supplementary Table S11 for Enrichment in NAC Synaptosomes; Supplementary Table S12 for Enrichment in DLPFC Synaptosomes. NAC nucleus accumbens, DLPFC dorsolateral prefrontal cortex.

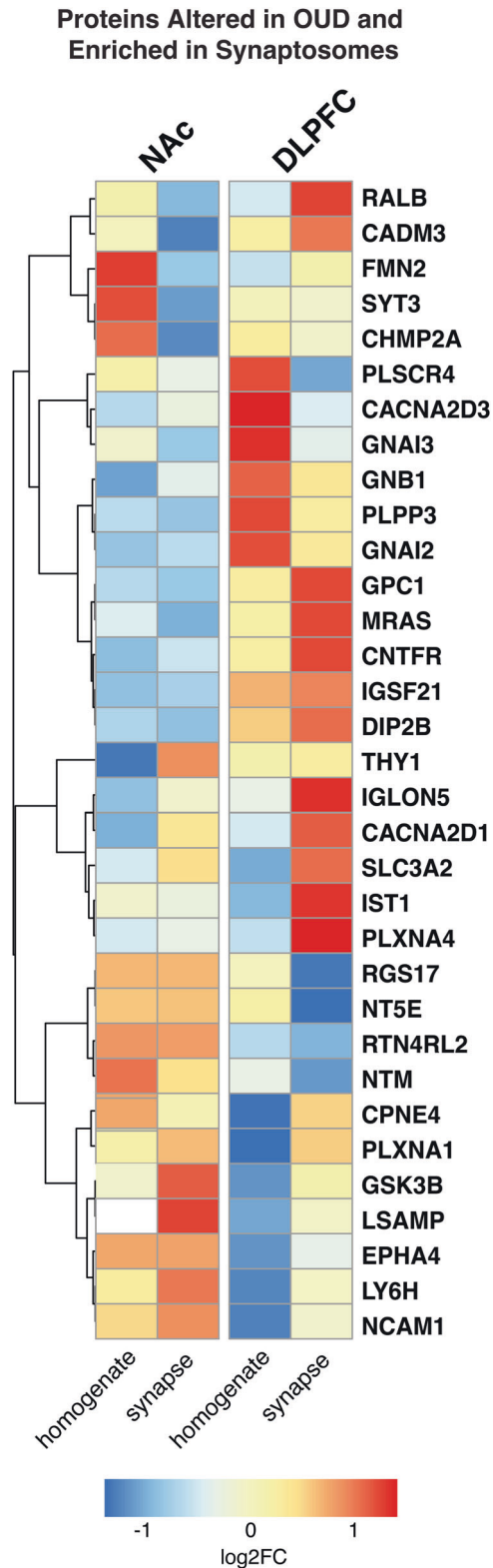


Fig. 3 Alterations in protein synaptic enrichments in DLPFC and NAc associated with OUD. Heatmap highlighting top differentially expressed proteins in homogenates and synaptosomes in NAc and DLPFC of OUD subjects compared to unaffected controls. Warmer colors indicate increasing \log_2FC and highly enriched proteins in OUD. In contrast, cooler colors indicate decreasing \log_2FC and negative enrichment of proteins in OUD synaptosomes. Proteins are filtered for $FDR < 0.10$.

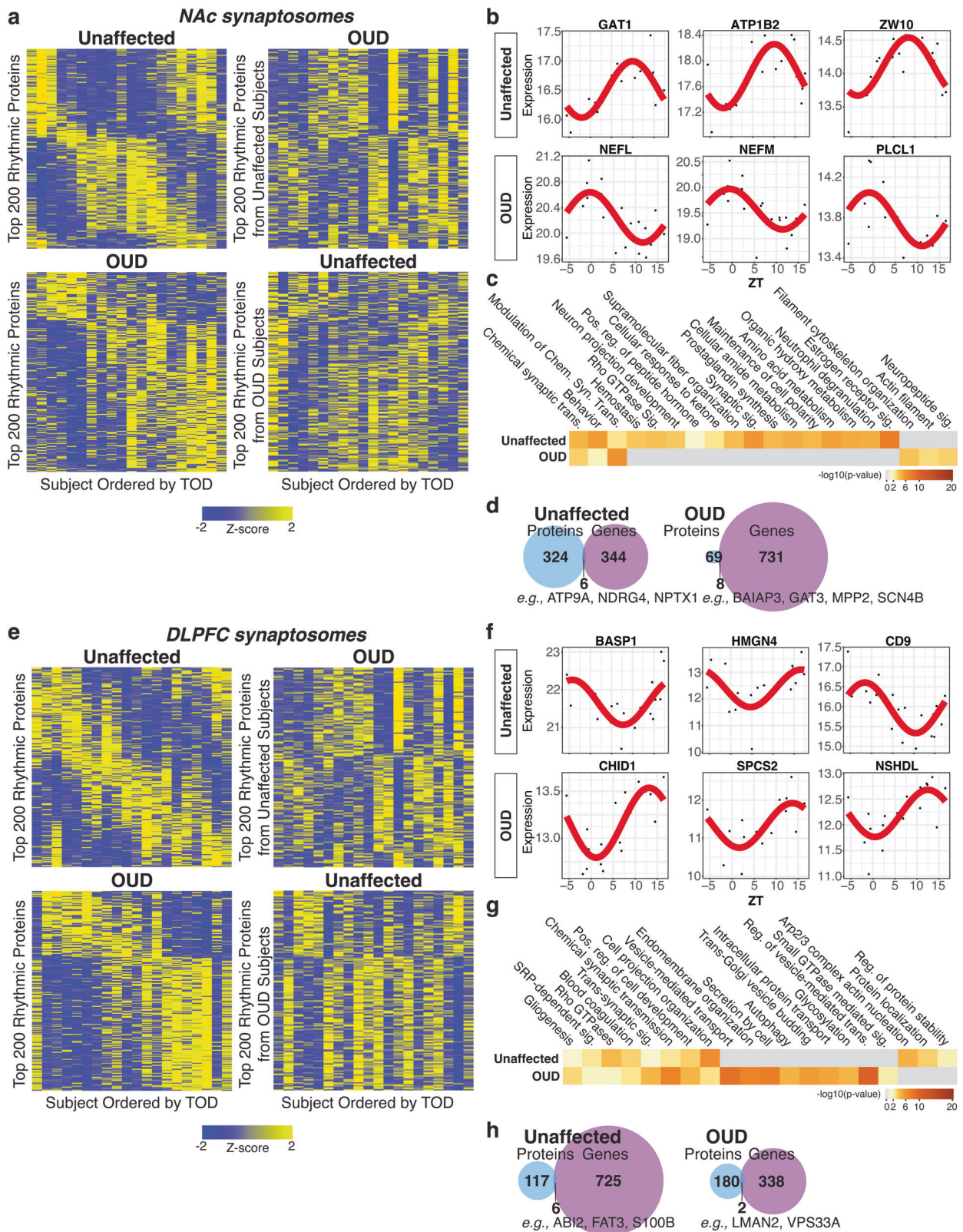
Additionally, we found similarly altered pathways in synaptosomes between brain regions. The major pathways enriched across NAc and DLPFC synaptosomes included morphine addiction and GABAergic signaling (e.g., GNG3, GABBR2, GNB1 in NAc; and GNAO1, GNB4, SLC6A11 in DLPFC), and glutamatergic synaptic signaling (e.g., GNG3, SLC1A3, and ADCY1 in NAc; and GNAO1, GNAS, and GNB14 in DLPFC; Fig. 2a, b).

Further investigation of the individual proteins enriched in synaptosomes revealed THY1 [64, 65], CACNA2D1 [66–70], SLC3A2 [70], GSK3B [71–73], LSAMP [73, 74], LY6H [75, 76], and NCAM1 [77–81], as the top synaptic proteins altered in NAc of OUD subjects (Fig. 3). In DLPFC, proteins altered in OUD and enriched in synaptosomes included RALB [82], CADM3 [83], GPC1 [84], MRAS, CNTFR [85], IGLON5, IST1, and PLXNA4 [86, 87] (Fig. 3). Other synapse-enriched proteins in DLPFC were like those enriched in NAc (e.g., GSK3B, LSAMP, NCAM1, CACNA2D1, SLC3A2; Fig. 3). Consistent with our pathway enrichments in synaptosomes of OUD subjects (Fig. 2), many of the synaptic proteins in both the NAc and DLPFC are involved in GABAergic and glutamatergic synaptic functions. For example, each of the synaptic proteins, CACNA2D1, SLC3A2, and GSK3B, altered in both brain regions, are known to dynamically regulate the activity of glutamatergic-dependent synaptic activity and plasticity [69, 70, 72].

Altered circadian rhythm signaling associated with OUD in synaptic proteomes of NAc and DLPFC

Previously, we reported transcriptional rhythm disruptions in NAc and DLPFC of subjects with OUD [2]. In support of this, a significantly enriched pathway in DE synaptic proteins in both brain regions were circadian entrainment (Fig. 2). Several preferentially enriched synaptic proteins have integral roles in the regulation of circadian rhythms (e.g., CACNA2D1, GSK3B, NCAM1, SYT3 [88]; Fig. 3). To further explore potential circadian rhythms in brain proteomes, we conducted TOD analysis on protein expression profiles from homogenate (Supplementary Fig. S2, Supplementary Fig. S1, Supplementary Tables S13–S20) and synaptosomes (Fig. 4a, b) of each brain region. In synaptosomes, we identified 300 and 77 significantly rhythmic proteins in NAc of unaffected and OUD subjects, respectively (Fig. 4d). In DLPFC synaptosomes, we identified 123 rhythmic proteins in unaffected and 182 rhythm proteins in OUD (Fig. 4h). Top rhythmic synaptic proteins in unaffected subjects were significantly disrupted in subjects with OUD across both brain regions in synaptosomes (Fig. 4a, e; Supplementary Tables S17–S20 and S23–S24) and homogenates (Supplementary Fig S2; Supplementary Tables S13–S16 and S21–S22). Vice-versa, we also found that proteins were only rhythmic in OUD compared to unaffected subjects. Consequently, top rhythmic proteins in OUD were different from rhythmic proteins in unaffected subjects in synaptosomes (Fig. 4a, NAc; Fig. 4e, DLPFC; Supplementary Tables S17–S20 and S23–S24) and homogenates (Supplementary Fig. S1; Supplementary Tables S13–S16 and S21–S22). These findings highlighted a gain in rhythmicity in OUD compared to unaffected subjects.

In NAc synaptosomes, the top rhythmic proteins of unaffected subjects included the GABA transporter, GAT1 [89, 90] (Fig. 4b). In OUD, top rhythmic proteins included neurofilament proteins (NEFL, NEFM [91]; Fig. 4b), consistent with enrichment of actin and filament cytoskeleton pathways (Fig. 4c). Neuropeptide signaling pathways were also enriched among rhythmic proteins in NAc of OUD subjects (Fig. 4c), a pathway that involves upstream initiation by G protein-coupled receptor binding to opioid receptors and downstream activation of intracellular pathways. Proteins encoding several opioid peptides were rhythmic in synaptosomes of OUD subjects, including PDYN (prodynorphin) and PENK (proenkephalin) [92, 93], and other proteins involved in opioid receptor signaling (SCG5 [94] and PCSK1N [95]). SCG5 and PCSK1N are also



secretory proteins involved in preventing the aggregation of proteins involved in neurodegenerative disorders.

In DLPFC synaptosomes, top rhythmic proteins of unaffected subjects included brain abundant membrane attached signal protein 1, *BASP1* (Fig. 4f). Moreover, *CHID1* [96] and *SPCS2* [97] were among the top rhythmic synaptic proteins in DLPFC of OUD

subjects (Fig. 4e, f), both of which are linked to cytoskeletal pathology in neurodegenerative disorders. Enrichment analyses of rhythmic synaptic proteins in DLPFC in OUD subjects revealed pathways primarily associated with Golgi and endoplasmic reticulum processing, autophagy, glycosylation, and synaptic vesicle transport (Fig. 4g). Disrupted endoplasmic reticulum

Fig. 4 Diurnal rhythms of protein expression in DLPFC and NAc synaptosomes associated with OUD. **a** Top left: Heatmap highlighting top 200 rhythmic proteins from NAc synaptosomes of unaffected subjects. Top right: Rhythmic proteins in unaffected subjects were plotted in OUD subjects to show disruption of protein rhythmicity. Bottom left: Heatmap highlighting top 200 rhythmic proteins from NAc synaptosomes of OUD subjects. Bottom right: rhythmic proteins in OUD subjects were plotted in unaffected subjects to show gain of protein rhythmicity in OUD. Heatmaps were generated by performing supervised clustering of expression of selected top 200 rhythmic proteins. Subjects were ordered by TOD to visualize expression levels over a period of 24 h. Yellow color indicates increased Z-score and higher protein expression, while blue color indicates decreased Z-score and lower protein expression. **b** Scatterplots of top rhythmic proteins in NAc synaptosomes from unaffected and OUD subjects. Scatterplots were generated to represent expression rhythms for individual proteins. The x-axis represents TOD on the ZT scale and protein expression level is on y-axis, with each dot representing a subject. The red line is the fitted sinusoidal curve to reflect temporal rhythms. **c** Pathway enrichment analysis comparing rhythmic proteins in NAc synaptosomes from unaffected and OUD subjects. Warmer colors indicate increasing $-\log_{10} p$ value and highly rhythmic pathways in each group. **d** Venn diagrams showing low overlap of rhythmic proteins and genes in NAc synaptosomes from unaffected and OUD subjects. **e** Top left: Heatmap highlighting top 200 rhythmic proteins from DLPFC synaptosomes of unaffected subjects. Top right: Rhythmic proteins in unaffected subjects were plotted in OUD subjects to show disruption of protein rhythmicity. Bottom left: heatmap highlighting top 200 rhythmic proteins from DLPFC synaptosomes of OUD subjects. Bottom right: rhythmic proteins in OUD subjects were plotted in unaffected subjects to show gain of protein rhythmicity in OUD. **f** Scatterplots of top rhythmic proteins in DLPFC synaptosomes from unaffected and OUD subjects. **g** Pathway enrichment analysis comparing top 200 rhythmic proteins found in DLPFC synaptosomes from unaffected and OUD subjects. **h** Venn diagrams showing low overlap of rhythmic proteins and genes in DLPFC synaptosomes from unaffected and OUD subjects. Also see Supplementary Fig. S1 for protein expression rhythm heatmaps in unaffected homogenates; Supplementary Fig. S2 for protein expression heatmaps in OUD homogenates; Supplementary Table S13 for NAc Homogenates Rhythms in Unaffected subjects; Supplementary Table S14 for NAc Homogenates Rhythms in OUD subjects; Supplementary Table S15 for DLPFC Homogenates Rhythms in Unaffected subjects; Supplementary Table S16 for DLPFC Homogenates Rhythms in OUD subjects; Supplementary Table S17 for NAc Synaptosomes Rhythms in Unaffected subjects; Supplementary Table S18 for NAc Synaptosomes Rhythms in OUD subjects; Supplementary Table S19 for DLPFC Synaptosomes Rhythms in Unaffected subjects; Supplementary Table S20 for DLPFC Synaptosomes Rhythms in OUD subjects; TOD time of death; NAc nucleus accumbens; DLPFC dorsolateral prefrontal cortex.

signaling, along with changes in the process of protein glycosylation, may reflect the impact of opioids on local protein translation and trafficking at postsynaptic sites, including dendritic spines, regulating synaptic plasticity [98].

In NAc homogenates of OUD subjects, top enriched pathways included opioid and synaptic signaling (Supplementary Fig. S2). DARPP32, a phosphoprotein critically involved in dopaminergic synaptic functions, was among the top rhythmic proteins in OUD (Supplementary Fig. S2). Rhythmic proteins specifically in NAc of OUD subjects were associated with pathways in various vesicle endocytotic processes (e.g., endocytosis, synaptic vesicle cycle, and clathrin-mediated endocytosis; Supplementary Fig. S2). In DLPFC, top rhythmic proteins in OUD subjects included the neurosecretory protein, VGF [99], and the putative negative regulator of cannabinoid receptor 1 activity, CNRIP1 (Supplementary Fig. S2). Top rhythmic pathways in OUD were related to glial cell development, mitochondrion organization, and various components of lipid and pyruvate metabolism (Supplementary Fig. S2). Rhythmicity in transcript abundance [2] was more prevalent compared to rhythms in protein expression in NAc and DLPFC (Supplementary Fig. S2). Notably, we observed very little overlap between rhythmic transcripts and rhythmic synaptic proteins (Fig. 4d, NAc; Fig. 4h, DLPFC) and homogenates (Supplementary Fig. S2) in either brain region of unaffected or OUD subjects.

Altered diurnal rhythms of the synaptic proteome in DLPFC and NAc associated with OUD

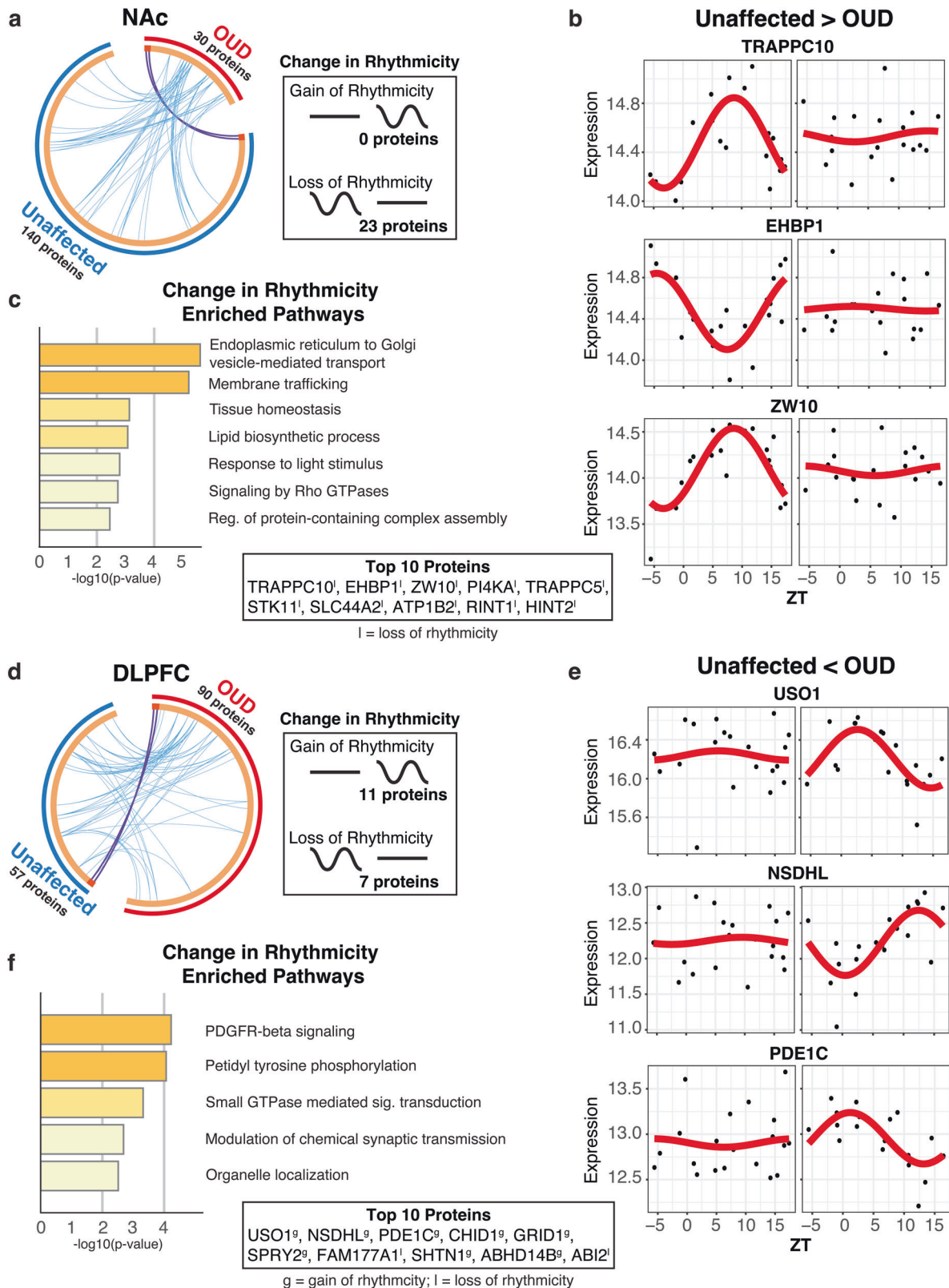
Rhythmic proteins were largely distinct between unaffected and OUD subjects across brain regions. Given this, we examined whether proteins lost or gained rhythms between unaffected and OUD subjects within each brain region and sample preparation (Homogenates: Supplementary Figs. S1–S3 and Supplementary Tables S21, S22; Synaptosomes: NAc, Fig. 5a; DLPFC, Fig. 5d; Supplementary Tables S23, S24). In NAc homogenates, 5 proteins lost rhythms and 19 proteins gained rhythms, primarily involved in protein translation (Supplementary Fig. S3a, S3c, Supplementary Table S21). Only 10 proteins were significantly altered in rhythmic expression in DLPFC homogenates of OUD subjects, with 3 proteins losing rhythms and 7 proteins gaining rhythms (Supplementary Fig. S3b). These proteins were enriched for pathways involved in lipid homeostasis and neurotoxicity, potentially related

to neurodegenerative processes (Supplementary Fig. 3d; Supplementary Table S22).

In synaptosomes, 23 proteins lost rhythmicity in NAc of OUD subjects (e.g., TRAPPC10, EHBPI, ZW10; Fig. 5a, b; Supplementary Table S23). Loss of protein rhythms in NAc were enriched for endoplasmic reticulum to Golgi vesicle-mediated transport pathways (Fig. 5c). In DLPFC, we found 7 synaptic proteins that lost rhythmicity in OUD and 11 synaptic proteins that gained rhythmicity (Fig. 5d; e.g., USO1, NSDHL, PDE1C [100], Fig. 5e). Proteins that gained rhythmicity (e.g., USO1, NSDHL, PDE1C, CHID1, GRID1) were involved in chemical synaptic transmission and organelle localization, while proteins that lost rhythmicity (e.g., FAM177A1, ABI2, TPD52L2, EIF2AK2, PRKCD) were involved in protein phosphorylation (Fig. 5f; Supplementary Table S24). Processed together, altered rhythmicity of synaptic proteins in DLPFC were associated with platelet-derived growth factor receptor beta (PDGFR-B) signaling (Fig. 5f), implicated in neuroprotection in response to elevated glutamatergic activity [101] and involved in opioid reward [102, 103]. Specifically, the 11 synaptic proteins gaining rhythmicity in DLPFC were associated with modulation of chemical synaptic transmission and organelle localization, while the 7 proteins losing rhythmicity were associated with protein phosphorylation (Supplementary Fig. S4; Supplementary Table S24). Collectively, our findings suggest circadian rhythm regulation of the synaptic proteome that is significantly altered in a brain region-specific manner in OUD. Further, circadian disruption of synaptic functions in OUD are associated with changes in endoplasmic reticulum-mediated local protein translation, trafficking, and vesicle endocytosis at the synapse, in addition to processes involved in neuroprotection and neurodegeneration.

Protein co-expression modules identify brain region-specific alterations in circadian rhythm signaling and synaptic functions associated with OUD

Using weighted co-expression analyses, we identified highly connected protein expression modules specific to NAc and DLPFC in homogenates (Supplementary Figs. S5, S7, S9; Supplementary Table S25) and synaptosomes (Supplementary Figs. S6, S8, S10; Supplementary Table S25). To further narrow modules relevant for OUD-associated protein alterations, we used MDC analysis, which examined the overall connectivity of protein co-expression and



network structure between unaffected and OUD subjects (Supplementary Table S26).

Many modules in unaffected subjects displayed a loss of connectivity in NAc and DLPFC homogenates (Supplementary Fig. S11; Supplementary Table S26) and synaptosomes (Fig. 6). In synaptosomes, connectivity was significantly lost in 13/15 modules

in the NAc of OUD subjects (Fig. 6a), along with 10/26 modules in DLPFC (Fig. 6b). Loss of connectivity in protein co-expression modules indicates significant dispersion of protein network structure related to OUD.

We then investigated whether modules with changes in connectivity were enriched for hub proteins specific to unaffected

Fig. 5 Altered rhythmicity of the synaptic proteome in DLPFC and NAc associated with OUD. Comparison of rhythmic proteins between unaffected and OUD subjects in synaptosomes from NAc and DLPFC. **a** Circoplots highlights few rhythmic proteins that were identical (purple lines) and shared ontology (light blue lines) between unaffected and OUD subjects in NAc synaptosomes. Change in rhythmicity analysis in NAc Synaptosomes revealed that 0 proteins gained rhythmicity, while 23 lost rhythmicity in OUD subjects. **b** Scatterplots of top proteins that lost rhythmicity in NAc synaptosomes between unaffected and OUD subjects. Scatterplots were generated to represent expression rhythms for individual proteins. The x-axis represents TOD on the ZT scale and protein expression level is on y-axis, with each dot representing a subject. The red line is the fitted sinusoidal curve to reflect temporal rhythms. **c** Pathway enrichment on proteins that changed rhythmicity between unaffected and OUD subjects in NAc synaptosomes. **d** Circoplots highlights few rhythmic proteins that were identical (purple lines) and shared ontology (light blue lines) between unaffected and OUD subjects in DLPFC synaptosomes. Change in rhythmicity analysis in DLPFC Synaptosomes revealed that 11 proteins gained rhythmicity, while 7 lost rhythmicity. **e** Scatterplots of top proteins that lost rhythmicity in DLPFC synaptosomes between unaffected and OUD subjects. **f** Pathway enrichment on proteins that changed rhythmicity between unaffected and OUD subjects in DLPFC synaptosomes. Also see Fig. S3 for gain/loss rhythmicity proteins in NAc and DLPFC homogenates; Supplementary Fig. S4 for DLPFC synaptosomes enriched gain and lost rhythm pathways; Table S21 for gain/loss rhythmicity protein list in NAc homogenates; Supplementary Table S22 for gain/loss rhythmicity protein list in DLPFC homogenates; Supplementary Table S23 for gain/loss rhythmicity protein list in NAc synaptosomes; Supplementary Table S24 for gain/loss rhythmicity protein list in DLPFC synaptosomes. TOD time of death, NAc nucleus accumbens, DLPFC dorsolateral prefrontal cortex.

and OUD subjects, and circadian rhythms. Focusing on the modules that lost connectivity in OUD, we found significant enrichment of both hub proteins specific to and/or rhythmic in unaffected subjects (Fig. 6). In NAc, there were three modules which lost connectivity in OUD that were significantly enriched for hub proteins (turquoise, green–yellow, and green; Fig. 6a). In the green module, proteins are associated with synaptic plasticity, dendritic spine formation, and axon guidance (e.g., ROCK2 [104], DPYSL5 [105, 106], PLAG1 [107, 108], GDAP1; Fig. 6a). In the green–yellow module, several of the rhythmic hub proteins were related to glutamatergic (GRIA2 [109, 110]), GABAergic (GABRA2 [111–113]), and calcium signaling (CAMK2B, CALB2) (Fig. 6a). Additionally, other hub proteins are involved in calcium signaling, membrane potential, glutamatergic signaling, and exocytosis of synaptic vesicles (rhythmic hub SCAMP5; hubs SYNGR3 and LRRF7; Fig. 6a). Overall, protein networks that lost connectivity in the NAc of OUD subjects were enriched for hub proteins that exhibited rhythmicity in unaffected subjects and involved in GABAergic and glutamatergic neurotransmission (Fig. 6c).

In DLPFC, we identified two modules that lost connectivity in OUD and with significant hub protein enrichments (Fig. 6b). The black module contained several highly connected hub proteins involved in ECM formation (LAMC1 [114]), presynaptic dopamine release (PLPP3 [115]), neuroprotection (NCEH1 [116], BCL2CL13), inflammation (LRRFIP2 [117]), and pronociceptive receptor signaling in pain (PIP5KL1 [118]). The green module contained several rhythmic hub proteins involved neuronal protection (NME3, SPHK2, RAB13), synaptic functions (MCTP1, NTNG2, GNG5), and transposon activity in the brain (PGBD5 [119]) (Fig. 6b). Enrichment analysis primarily highlighted synaptic functions of vesicle cycling and structure (Fig. 6d). Collectively, our analyses lend further support for a role of circadian rhythms in synaptic signaling within human brain and suggest significant disruptions of circadian-dependent regulation of synaptic functions in OUD.

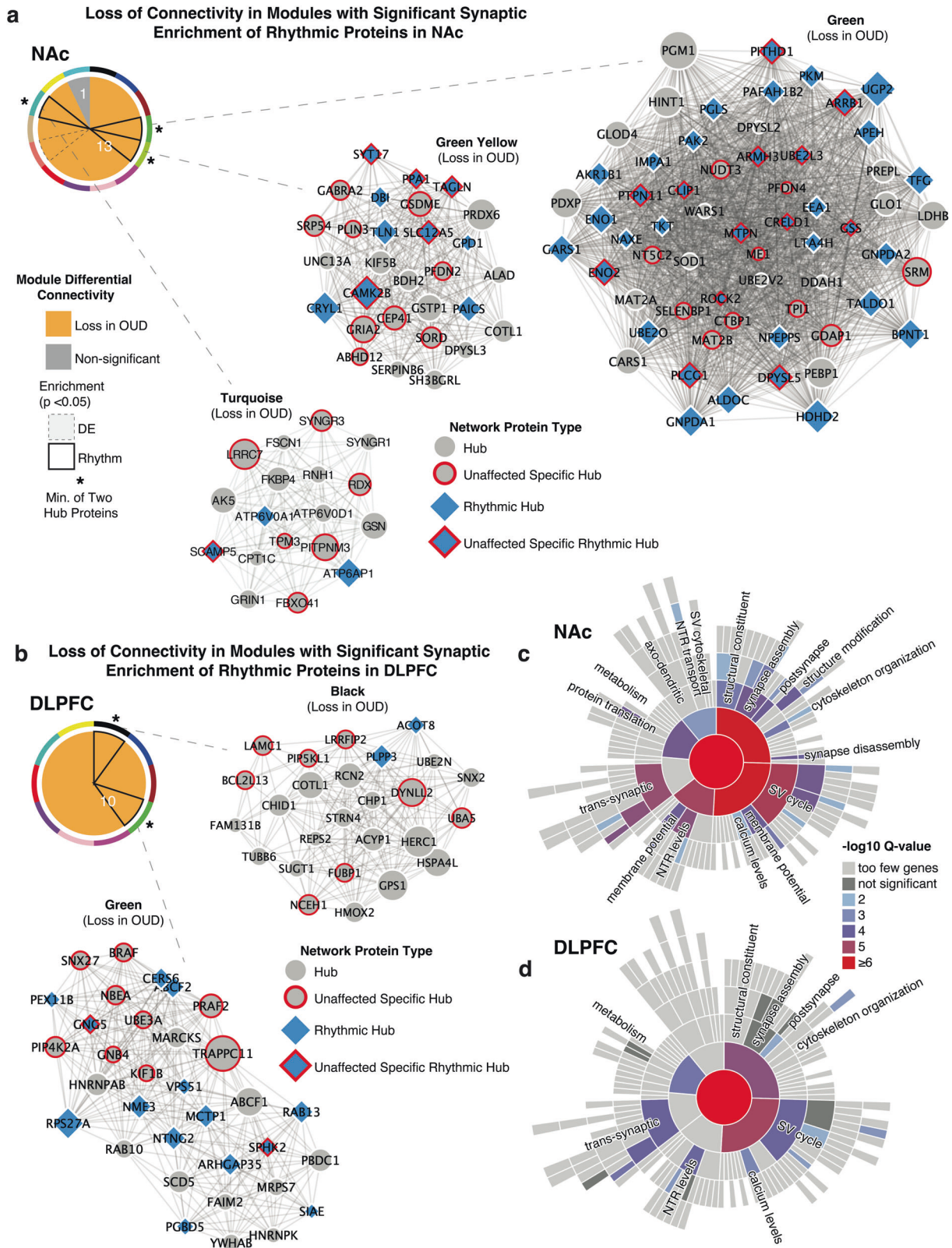
DISCUSSION

Our previous transcriptomic findings implicate circadian rhythm disruption in proinflammatory signaling and synaptic remodeling in human NAc and DLPFC in OUD [2, 3]. We extend these findings here by showing significant alterations in circadian rhythm, GABAergic, and glutamatergic synaptic processes in both regions of the same OUD subjects. Using high-density profiling of peptides in tissue homogenates and synaptosomes within brain regions from the same subjects, we were able to identify and parse significant OUD-associated changes in synaptic proteomes specific to and common to NAc and DLPFC. In NAc synaptosomes specifically, pathways were involved in inflammatory, mitochondria, and metabolic signaling. In DLPFC synaptosomes from OUD subjects, pathways were mainly related to significant alterations in inflammatory signaling and serotonergic, dopaminergic, cholinergic, oxytocin

neurotransmission. In both brain regions, pathways related to neurodegeneration, GABAergic and glutamatergic synapses, and circadian rhythms were associated with OUD, further supporting a role for circadian rhythms in synaptic signaling in opioid addiction.

Alterations in protein pathways related to neurodegeneration in OUD subjects were common in both NAc and DLPFC homogenates and synaptosomes. The relationship between chronic opioid use and increased risk for neurodegenerative disorders is complex. Several studies have reported increased risk of dementia and higher incidence of neurodegenerative disorders in people with heavy, chronic opioid use [120–122]. Chronic opioid use and dysfunction of the opioid system in the brain may contribute to neuroinflammation and the hyperphosphorylation of tau, a key protein involved in the pathogenesis of Alzheimer's disease [122]. For example, dysfunction of opioid receptor signaling leads to increased amyloid beta expression and deposition [120]. Accumulation of amyloid beta is involved in the neurotoxicity observed early in the development of Alzheimer's disease.

Consistent with the emergence of early pathogenesis associated with neurodegenerative disorders, several studies have shown significant elevation of early markers of neuropathology in Alzheimer's disease in subjects who chronically used heroin, including hyperphosphorylated tau and amyloid beta [122]. Neurodegenerative markers in the brain were positively correlated with neuroinflammatory markers and microglial activation. Intriguingly, levels of the enzyme that phosphorylates tau, GSK3B, were also increased in the same subjects [122]. We identified GSK3B as a synaptic-enriched protein significantly upregulated in NAc and to a lesser degree in DLPFC of OUD subjects. Other related proteins were changed in both regions, including reduced expression of CBR1, BIN1, and VPS29 in DLPFC synaptosomes and reduced expression of SIRT2 in NAc synaptosomes. CBR1 is usually elevated in response to neuroinflammation and neuronal injury, ultimately facilitating neuroprotection [123]. Reduced BIN1 expression and function is a known risk factor for late-onset Alzheimer's disease, having critical roles in presynaptic release of glutamate and the facilitation of learning and memory [124]. Further, VPS29 is involved in synaptic survival [125]. OUD-associated downregulation of each of these proteins in DLPFC may reflect the initiation of molecular signaling cascades resembling early pathogenesis of Alzheimer's disease. In addition, SIRT2 downregulation in NAc synapses could lead to augmented activity at excitatory synapses via dysfunction of AMPA and NMDA glutamate receptors [126, 127]. Accumulation of phosphorylated tau and other markers of neurodegenerative diseases, accompanied by elevated neuroinflammation in the brain, likely have functional impacts on synaptic processes in NAc and DLPFC in OUD. In OUD, several synaptic proteins were enriched in both NAc and DLPFC that link neurotoxicity to augmented glutamatergic neurotransmission—CNTFR, PLXNA4, and SLC3A2. Although speculative, alterations in synaptic processes we highlighted here



in subjects with OUD, particularly GABAergic and glutamatergic neurotransmission, may be associated with cognitive, mood, and reward dysfunction associated with opioid addiction.

An imbalance of GABAergic and glutamatergic signaling in NAc and DLPFC has been linked to OUD and other psychiatric disorders. Between NAc and DLPFC of OUD subjects, our analyses

identified several of the most impacted pathways in synapses including GABAergic and glutamatergic neurotransmission. Several notable proteins involved in glutamatergic excitatory synapses were upregulated in DLPFC synaptosomes—GRIN2A (glutamate ionotropic receptor NMDA type subunit 2A), GRIN2B (glutamate ionotropic receptor NMDA type subunit 2B), GRM1

Fig. 6 Altered protein networks in NAc and DLPFC synaptosomes associated with OUD. Weight Gene Correlation Network Analysis (WGCNA) was used to generate protein co-expression modules from each brain region separately. The identified modules that survived module preservation analysis were arbitrarily assigned colors. Pie charts generated from module differential connectivity (MDC) analysis summarize modules that gained or lost connectivity between unaffected and OUD subjects in NAc (**a**) and DLPFC (**b**). **a** Comparing module connectivity between unaffected and OUD subjects in NAc synaptosomes identified 13 modules that lost connectivity in OUD, while 1 remained unchanged. Modules turquoise, green–yellow and green were composed of several rhythmic protein hubs and showed loss in connectivity in OUD. **b** Comparing module connectivity between unaffected and OUD subjects in DLPFC synaptosomes revealed all identified modules lost connectivity in OUD. Modules Green and Black were composed of several rhythmic hubs and showed loss of connectivity in OUD. **c** Synaptic enrichment analysis of protein networks that lost connectivity in NAc synaptosomes. **d** Synaptic enrichment analysis of protein networks that lost connectivity in DLPFC synaptosomes. Also see Figure S5 for WGCNA dendrograms on NAc and DLPFC homogenates; Fig. S6 for WGCNA dendrograms on NAc and DLPFC synaptosomes; Figure S7 for modules from NAc homogenates; Fig. S8 for modules from NAc synaptosomes; Figure S9 for modules from DLPFC homogenates; Fig. S10 for modules from DLPFC synaptosomes; Fig. S11 for additional MDC summaries; Supplementary Table S25 for WGCNA module assignments and proteins; Supplementary Table S26 for MDC analysis. DE differentially expressed, NAc nucleus accumbens, DLPFC dorsolateral prefrontal cortex.

(glutamate metabotropic receptor 1), and SHANK2 (SH3 and multiple ankyrin repeat domains 2). GRIN proteins are subunits of the NMDA receptor complex, both of which are intimately involved in opioid-induced excitatory synaptic plasticity, having integral roles in opioid withdrawal and craving [128–130]. Synaptic elevation of SHANK2 may elevate NMDA receptor activity and enhance bursting of parvalbumin-positive neurons in DLPFC [131]. Enhancing NMDA receptor activation impairs synaptic plasticity and leads to cognitive impairments, potentially involved in OUD. We identified other synapse-specific proteins in the NAc involved in NMDA-dependent glutamate signaling, such as FLOT2 (upregulated), HDAC11 (downregulated), and SLC18B1 (downregulated). Notably, reduced HDAC11 expression in OUD and function may impede synaptic plasticity [132]. CACNA2D1, SLC3A2, and GSK3B, among others, were also enriched in both NAc and DLPFC of OUD subjects, each of which have dynamic roles in the regulation of glutamatergic-dependent synaptic plasticity. In addition, proteins involved in GABAergic processes were also significantly altered in OUD. For example, GAD2 was reduced in DLPFC synaptosomes in subjects with OUD. GAD2 is associated with synaptic vesicle response during intense neuronal activity to release GABA into the synaptic cleft [133], consistent with dysfunctional inhibitory neurotransmission in opioid addiction.

Additionally, we identified proteins specifically altered in NAc and DLPFC of OUD subjects. For example, LSAMP and LY6H were more enriched in NAc synaptosomes, both of which are involved in dendritic spine formation in response to excitatory inputs. Other proteins related to neuroinflammation were upregulated in NAc (e.g., HLA-B, GSTT1, S100A9). In DLPFC, synaptic-enriched proteins included IGLON5, a neuronal adhesion molecule linked to neurological disorder characterized by sleep disorders and cognitive impairments; EPHA4 [134], a receptor tyrosine kinase that modulates aberrant synaptic functions in response to neuronal injury and neuroinflammation; and GPC1, a glycoprotein involved in extracellular matrix (ECM) formation. Several proteins with the highest fold-change in OUD subjects included keratin cytoskeletal, ECM-related proteins in NAc [135]. Reduced expression and function of keratin proteins and neurofilaments are associated with neuropsychiatric disorders [121, 122], including stress-related disorders and substance use disorders [46]. The co-occurrence of changes in proteins involved in the activation of neuroinflammatory processes, degradation of ECM, and synaptic remodeling corroborates our previous transcriptomic findings in opioid addiction [3].

Pathway analysis implicated circadian rhythm disruption primarily in synaptosomes of OUD subjects. However, protein expression rhythms were markedly disrupted in both homogenates and synaptosomes from NAc and DLPFC. For example, DARPP-32, a protein highly expressed in striatal medium spiny neurons [136–138], was highly rhythmic in NAc homogenates, suggesting opioid-induced circadian reprogramming of molecular cascades in the striatum [139]. Notably, opioid signaling was a top pathway that was rhythmic in NAc homogenates, where rhythms

in opioid neurotransmission may contribute to craving and relapse [140, 141]. Proteins that lost rhythmicity in the NAc of OUD subjects were involved in membrane trafficking and endoplasmic reticulum to Golgi vesicle-mediated transport (e.g., TRAPPC5, TRAPPC10, EHBP1, ZW10). Both TRAPPC5 and TRAPPC10 are transmembrane proteins of the cis-Golgi complex that support vesicular transport from endoplasmic reticulum to Golgi. TRAPP10 interacts with TRAPPC9 to form TRAPP II core proteins. TRAPPC9/10 proteins regulate the endocytic receptor recycling of dopamine 1 and 2 receptors in postsynaptic striatal medium spiny neurons [142], integral to regulation of medium spiny neuron physiology and motivated behaviors. Local translation at synaptic sites may also occur through activity-dependent transport [143]. Glycoproteins THY1 and NCAM1 [144] were highly rhythmic in DLPFC homogenates. An area of future work could explore the impact of opioids on protein glycosylation of synaptic proteins and their impact of synaptic vesicle loading and release, particularly glutamate receptor turnover and activation [145] in response to neuroinflammation [146, 147]. In addition, PDGFR-B signaling was among the top pathways from altered rhythms in protein expression of DLPFC synaptosomes in OUD. Importantly, PDGF-dependent signaling is involved in numerous opioid actions, including tolerance and reward [148]. PDGF is a receptor tyrosine kinase, suggesting interactions between tyrosine kinases and opioid receptors may directly modulate glutamate receptor activity [149] depending on their circadian regulation.

Co-expression analyses revealed further insights into the role of circadian rhythm regulation of synaptic dysfunction in OUD. We identified several protein modules that were enriched for rhythmic proteins and hub proteins involved in synaptic processes in unaffected subjects (e.g., CAMK2B, GSK3B, ROCK2, PLCG1, SCAMP5, SYT17). Each of which are involved in dendritic spine formation and synaptic plasticity [104]. Every highly connected module in unaffected subjects in NAc and DLPFC lost connectivity in OUD subjects. Loss of connectivity in these protein networks in OUD could resemble a lack of coordinated protein signaling at the synapse that is modulated by circadian rhythms. OUD-associated upregulation of GSK3B in synaptosomes of NAc and DLPFC likely leads to significant molecular rhythm disruptions in synapses, with potential consequences on activity-dependent synaptic plasticity, and thus, may be a lynchpin in opioid and circadian actions at the synapse.

Overall, our findings implicate circadian rhythm disruption in altered functions at GABAergic and glutamatergic synapses in both NAc and DLPFC. Considering the role of sleep and circadian rhythms in opioid reward, craving, and relapse, treatments that target circadian pathways may be an effective therapeutic strategy for OUD.

REFERENCES

1. National Institute on Drug Abuse. Drug overdose death rates. National Institute on Drug Abuse; 2023. <https://nida.nih.gov/research-topics/trends-statistics/overdose-death-rates>. Accessed 23 March 2023.

2. Xue X, Zong W, Glausier JR, Kim S-M, Shelton MA, Phan BN, et al. Molecular rhythm alterations in prefrontal cortex and nucleus accumbens associated with opioid use disorder. *Transl Psychiatry*. 2022;12:1–13.
3. Seney ML, Kim S-M, Glausier JR, Hildebrand MA, Xue X, Zong W, et al. Transcriptional alterations in dorsolateral prefrontal cortex and nucleus accumbens implicate neuroinflammation and synaptic remodeling in opioid use disorder. *Biol Psychiatry*. 2021;90:550–62.
4. Nagamatsu ST, Rompala G, Hurd YL, Núñez-Ríos DL, Montalvo-Ortiz JL, Traumatic Stress Brain Research Group. CpH methylome analysis in human cortical neurons identifies novel gene pathways and drug targets for opioid use disorder. *Front Psychiatry*. 2022;13:1078894.
5. Jacobs MM, Ökvist A, Horvath M, Keller E, Bannon MJ, Morgello S, et al. Dopamine receptor D1 and postsynaptic density gene variants associate with opiate abuse and striatal expression levels. *Mol Psychiatry*. 2013;18:1205–10.
6. Sullivan SE, Whittard JD, Jacobs MM, Ren Y, Mazloom AR, Caputi FF, et al. ELK1 transcription factor linked to dysregulated striatal mu opioid receptor signaling network and OPRM1 polymorphism in human heroin abusers. *Biol Psychiatry*. 2013;74:511–9.
7. Brown TG, Xu J, Hurd YL, Pan Y-X. Dysregulated expression of the alternatively spliced variant mRNAs of the mu opioid receptor gene, OPRM1, in the medial prefrontal cortex of male human heroin abusers and heroin self-administering male rats. *J Neurosci Res*. 2022;100:35–47.
8. Valeri J, O'Donovan SM, Wang W, Sinclair D, Bollavarapu R, Gisabella B, et al. Altered expression of somatostatin signaling molecules and clock genes in the hippocampus of subjects with substance use disorder. *Front Neurosci*. 2022;16:903941.
9. Grimm SL, Mendez EF, Stertz L, Meyer TD, Fries GR, Gandhi T, et al. MicroRNA-mRNA networks are dysregulated in opioid use disorder postmortem brain: further evidence for opioid-induced neurovascular alterations. *Front Psychiatry*. 2022;13:1025346.
10. Mendez EF, Wei H, Hu R, Stertz L, Fries GR, Wu X, et al. Angiogenic gene networks are dysregulated in opioid use disorder: evidence from multi-omics and imaging of postmortem human brain. *Mol Psychiatry*. 2021;26:7803–12.
11. Baldo BA. Prefrontal cortical opioids and dysregulated motivation: a network hypothesis. *Trends Neurosci*. 2016;39:366–77.
12. Adinoff B, Rilling LM, Williams MJ, Schreffler E, Schepis TS, Rosvall T, et al. Impulsivity, neural deficits, and the addictions: the 'oops' factor in relapse. *J Addict Dis*. 2007;26:25–39.
13. Koob GF. Neurobiology of opioid addiction: opponent process, hyperkatifeia, and negative reinforcement. *Biol Psychiatry*. 2020;87:44–53.
14. Mahfoud Y, Talih F, Stroom D, Budur K. Sleep disorders in substance abusers: how common are they? *Psychiatry Edgmont Pa Townsh*. 2009;6:38–42.
15. Huhn AS, Ellis JD, Dunn KE, Sholler DJ, Tabaschek P, Burns R, et al. Patient-reported sleep outcomes in randomized-controlled trials in persons with substance use disorders: a systematic review. *Drug Alcohol Depend*. 2022;237:109508.
16. Huhn AS, Finan PH, Gamaldo CE, Hammond AS, Umbricht A, Bergeria CL, et al. Suvorexant ameliorated sleep disturbance, opioid withdrawal, and craving during a buprenorphine taper. *Sci Transl Med*. 2022;14:eabn8238.
17. Eacret D, Veasey SC, Blendy JA. Bidirectional relationship between opioids and disrupted sleep: putative mechanisms. *Mol Pharmacol*. 2020;98:445–53.
18. Eacret D, Manduchi E, Noreck J, Tyner E, Fenik P, Dunn AD, et al. Mu-opioid receptor-expressing neurons in the paraventricular thalamus modulate chronic morphine-induced wake alterations. *Transl Psychiatry*. 2023;13:78.
19. Oyefeso A, Sedgwick P, Ghodse H. Subjective sleep-wake parameters in treatment-seeking opiate addicts. *Drug Alcohol Depend*. 1997;48:9–16.
20. Stinus L, Robert C, Karasinski P, Limoge A. Continuous quantitative monitoring of spontaneous opiate withdrawal: locomotor activity and sleep disorders. *Pharmacol Biochem Behav*. 1998;59:83–9.
21. Li S, Shi J, Epstein DH, Wang X, Zhang X, Bao Y, et al. Circadian alteration in neurobiology during 30 days of abstinence in heroin users. *Biol Psychiatry*. 2009;65:905–12.
22. Cao M, Javaheri S. Effects of chronic opioid use on sleep and wake. *Sleep Med Clin*. 2018;13:271–81.
23. McClatchy DB, Liao L, Park SK, Venable JD, Yates JR. Quantification of the synaptosomal proteome of the rat cerebellum during post-natal development. *Genome Res*. 2007;17:1378–88.
24. MacDonald ML, Garver M, Newman J, Sun Z, Kannarkat J, Salisbury R, et al. Synaptic proteome alterations in the primary auditory cortex of individuals with schizophrenia. *JAMA Psychiatry*. 2020;77:86–95.
25. Carney KE, Milanese M, van Nierop P, Li KW, Oliet SHR, Smit AB, et al. Proteomic analysis of gliosomes from mouse brain: identification and investigation of glial membrane proteins. *J Proteome Res*. 2014;13:5918–27.
26. Dumrongprechachan V, Salisbury RB, Butler L, MacDonald ML, Kozorovitskiy Y. Dynamic proteomic and phosphoproteomic atlas of corticostriatal axons in neurodevelopment. *ELife* 2022;11:e78847.
27. Dumrongprechachan V, Salisbury RB, Soto G, Kumar M, MacDonald ML, Kozorovitskiy Y. Cell-type and subcellular compartment-specific APEX2 proximity labeling reveals activity-dependent nuclear proteome dynamics in the striatum. *Nat Commun*. 2021;12:4855.
28. Glausier JR, Kelly MA, Salem S, Chen K, Lewis DA. Proxy measures of premortem cognitive aptitude in postmortem subjects with schizophrenia. *Psychol Med*. 2020;50:507–14.
29. Volk DW, Matsubara T, Li S, Sengupta EJ, Georgiev D, Minabe Y, et al. Deficits in transcriptional regulators of cortical parvalbumin neurons in schizophrenia. *Am J Psychiatry*. 2012;169:1082–91.
30. Hashimoto T, Bazmi HH, Mirnics K, Wu Q, Sampson AR, Lewis DA. Conserved regional patterns of GABA-related transcript expression in the neocortex of subjects with schizophrenia. *Am J Psychiatry*. 2008;165:479–89.
31. Hahn C-G, Banerjee A, Macdonald ML, Cho D-S, Kamins J, Nie Z, et al. The postsynaptic density of human postmortem brain tissues: an experimental study paradigm for neuropsychiatric illnesses. *PLoS ONE*. 2009;4:e5251.
32. MacDonald ML, Ciccimaro E, Prakash A, Banerjee A, Seeholzer SH, Blair IA, et al. Biochemical fractionation and stable isotope dilution liquid chromatography-mass spectrometry for targeted and microdomain-specific protein quantification in human postmortem brain tissue. *Mol Cell Proteom*. 2012;11:1670–81.
33. Zecha J, Satpathy S, Kanashova T, Avanesian SC, Kane MH, Clauser KR, et al. TMT labeling for the masses: a robust and cost-efficient, in-solution labeling approach. *Mol Cell Proteom*. 2019;18:1468–78.
34. Perez-Riverol Y, Bai J, Bandla C, García-Seisdedos D, Hewapathirana S, Kamatchinathan S, et al. The PRIDE database resources in 2022: a hub for mass spectrometry-based proteomics evidences. *Nucleic Acids Res*. 2021;50:D543–52.
35. Browne CJ, Futamura R, Minier-Toribio A, Hicks EM, Ramakrishnan A, Martínez-Rivera F, et al. Transcriptional signatures of heroin intake and seeking throughout the brain reward circuit. 2023. <https://doi.org/10.1101/2023.01.11.523688>.
36. Mews P, Cunningham AM, Scarpa J, Ramakrishnan A, Hicks EM, Bolnick S, et al. Convergent abnormalities in striatal gene networks in human cocaine use disorder and mouse cocaine administration models. *Sci Adv*. 2023;9:eadd8946.
37. Yu G, Wang L-G, Han Y, He Q-Y. clusterProfiler: an R package for comparing biological themes among gene clusters. *Omics J Integr Biol*. 2012;16:284–7.
38. Yu G, He Q-Y. ReactomePA: an R/Bioconductor package for reactome pathway analysis and visualization. *Mol Biosyst*. 2016;12:477–9.
39. Zhou Y, Zhou B, Pache L, Chang M, Khodabakhshi AH, Tanaseichuk O, et al. Metascape provides a biologist-oriented resource for the analysis of systems-level datasets. *Nat Commun*. 2019;10:1523.
40. Langfelder P, Horvath S. WGCNA: an R package for weighted correlation network analysis. *BMC Bioinforma*. 2008;9:559.
41. Langfelder P, Zhang B, Horvath S. Defining clusters from a hierarchical cluster tree: the Dynamic Tree Cut package for R. *Bioinformatics*. 2008;24:719–20.
42. Zhang B, Horvath S. A general framework for weighted gene co-expression network analysis. *Stat Appl Genet Mol Biol*. 2005;4:Article17.
43. Margolin AA, Nemenman I, Basso K, Wiggins C, Stolovitzky G, Dalla Favera R, et al. ARACNE: an algorithm for the reconstruction of gene regulatory networks in a mammalian cellular context. *BMC Bioinforma*. 2006;7:57.
44. Koopmans F, van Nierop P, Andres-Alonso M, Byrnes A, Cijssouw T, Coba MP, et al. SynGO: an evidence-based, expert-curated knowledge base for the synapse. *Neuron*. 2019;103:217–34.e4.
45. Cahill KM, Huo Z, Tseng GC, Logan RW, Seney ML. Improved identification of concordant and discordant gene expression signatures using an updated rank-rank hypergeometric overlap approach. *Sci Rep*. 2018;8:9588.
46. Morrison KE, Stenson AF, Marx-Rattner R, Carter S, Michopoulos V, Gillespie CF, et al. Developmental timing of trauma in women predicts unique extracellular vesicle proteome signatures. *Biol Psychiatry*. 2022;91:273–82.
47. Javitt A, Barnea E, Kramer MP, Wolf-Levy H, Levin Y, Admon A, et al. Pro-inflammatory cytokines alter the immunopeptidome landscape by modulation of HLA-B expression. *Front Immunol*. 2019;10.
48. Liang TW, Chiu HH, Gurney A, Sidle A, Tumas DB, Schow P, et al. Vascular endothelial-junctional adhesion molecule (VE-JAM)/JAM 2 interacts with T, NK, and dendritic cells through JAM 3. *J Immunol*. 2002;168:1618–26.
49. Koss H, Bunney TD, Behjati S, Katan M. Dysfunction of phospholipase C γ in immune disorders and cancer. *Trends Biochem Sci*. 2014;39:603–11.
50. Sabbir MG, Speth RC, Albensi BC. Loss of Cholinergic Receptor Muscarinic 1 (CHRM1) protein in the hippocampus and temporal cortex of a subset of individuals with Alzheimer's disease, Parkinson's disease, or frontotemporal dementia: implications for patient survival. *J Alzheimers Dis* 2022;90:727–47.
51. Zhu G, Fang Y, Cui X, Jia R, Kang X, Zhao R. Magnolol upregulates CHRM1 to attenuate Amyloid- β -triggered neuronal injury through regulating the cAMP/PKA/CREB pathway. *J Nat Med*. 2022;76:188–99.
52. Strang KH, Golde TE, Giasson BI. MAPT mutations, tauopathy, and mechanisms of neurodegeneration. *Lab Invest*. 2019;99:912–28.

53. Ma S, Attarwala IY, Xie X-Q. SQSTM1/p62: a potential target for neurodegenerative disease. *ACS Chem Neurosci*. 2019;10:2094–114.
54. Aykac A, Sehirli AO. The role of the SLC transporters protein in the neurodegenerative disorders. *Clin Psychopharmacol Neurosci*. 2020;18:174–87.
55. Chee LY, Cumming A. Polymorphisms in the cholinergic receptors muscarinic (CHRM2 and CHRM3) genes and Alzheimer's disease. *Avicenna J Med Biotechnol*. 2018;10:196–9.
56. Querfurth H, Lee H-K. Mammalian/mechanistic target of rapamycin (mTOR) complexes in neurodegeneration. *Mol Neurodegener*. 2021;16:44.
57. Foskett JK. Inositol trisphosphate receptor Ca²⁺ release channels in neurological diseases. *Pflug Arch*. 2010;460:481–94.
58. Lokireddy S, Kukushkin NV, Goldberg AL. cAMP-induced phosphorylation of 26S proteasomes on Rpn6/PSMD11 enhances their activity and the degradation of misfolded proteins. *Proc Natl Acad Sci USA*. 2015;112:E7176–85.
59. Huang Z-N, Her L-S. The ubiquitin receptor ADRM1 modulates HAP40-Induced Proteasome Activity. *Mol Neurobiol*. 2017;54:7382–7400.
60. Benkler C, O'Neil AL, Slepian S, Qian F, Weinreb PH, Rubin LL. Aggregated SOD1 causes selective death of cultured human motor neurons. *Sci Rep*. 2018;8:16393.
61. Heremans IP, Caligiore F, Gerin I, Bury M, Lutz M, Graff J, et al. Parkinson's disease protein PARK7 prevents metabolite and protein damage caused by a glycolytic metabolite. *Proc Natl Acad Sci USA*. 2022;119:e2111338119.
62. Plun-Favreau H, Klupsch K, Moisoï N, Gandhi S, Kjaer S, Frith D, et al. The mitochondrial protease Htra2 is regulated by Parkinson's disease-associated kinase PINK1. *Nat Cell Biol*. 2007;9:1243–52.
63. Shi Q, Li J-L, Ma Y, Gao L-P, Xiao K, Wang J, et al. Decrease of Ryr2 in the prion infected cell line and in the brains of the scrapie infected mice models and the patients of human prion diseases. *Prion*. 2018;12:175–84.
64. Bradley JA, Ramirez G, Hagood JS. Roles and regulation of Thy-1, a context-dependent modulator of cell phenotype. *BioFactors*. 2009;35:258–65.
65. Jeng C-J, McCarroll SA, Martin TFJ, Floor E, Adams J, Krantz D, et al. Thy-1 is a component common to multiple populations of synaptic vesicles. *J Cell Biol*. 1998;140:685–98.
66. Dahimene S, von Elsner L, Holling T, Mattas LS, Pickard J, Lessel D, et al. Biallelic CACNA2D1 loss-of-function variants cause early-onset developmental epileptic encephalopathy. *Brain J Neurol*. 2022;145:2721–9.
67. Grosso BJ, Kramer AA, Tyagi S, Bennett DF, Tiffit CJ, D'Souza P, et al. Complex effects on Cav2.1 channel gating caused by a CACNA1A variant associated with a severe neurodevelopmental disorder. *Sci Rep*. 2022;12:9186.
68. Luo X, Rosenfeld JA, Yamamoto S, Harel T, Zuo Z, Hall M, et al. Clinically severe CACNA1A alleles affect synaptic function and neurodegeneration differentially. *PLoS Genet*. 2017;13:e1006905.
69. Chen J, Li L, Chen S-R, Chen H, Xie J-D, Sirrieh RE, et al. The $\alpha 2\delta$ -1-NMDA receptor complex is critically involved in neuropathic pain development and gabapentin therapeutic actions. *Cell Rep*. 2018;22:2307–21.
70. Lin C-H, Lin P-P, Lin C-Y, Lin C-H, Huang C-H, Huang Y-J, et al. Decreased mRNA expression for the two subunits of system xc⁻, SLC3A2 and SLC7A11, in WBC in patients with schizophrenia: evidence in support of the hypo-glutamatergic hypothesis of schizophrenia. *J Psychiatr Res*. 2016;72:58–63.
71. Peineau S, Bradley C, Taghibiglou C, Doherty A, Bortolotto ZA, Wang YT, et al. The role of GSK-3 in synaptic plasticity. *Br J Pharmacol*. 2008;153:5428–37.
72. Jaworski T, Banach-Kasper E, Gralec K. GSK-3 β at the intersection of neuronal plasticity and neurodegeneration. *Neural Plast*. 2019;2019:4209475.
73. Bregin A, Kaare M, Jagom e T, Karis K, Singh K, Laugus K, et al. Expression and impact of Lsamp neural adhesion molecule in the serotonergic neurotransmission system. *Pharmacol Biochem Behav*. 2020;198:173017.
74. Bregin A, Mazitov T, Aug I, Philips M-A, Innos J, Vasar E. Increased sensitivity to psychostimulants and GABAergic drugs in Lsamp-deficient mice. *Pharmacol Biochem Behav*. 2019;183:87–97.
75. Moriwaki Y, Kubo N, Watanabe M, Asano S, Shinoda T, Sugino T, et al. Endogenous neurotoxin-like protein Ly6H inhibits $\alpha 7$ nicotinic acetylcholine receptor currents at the plasma membrane. *Sci Rep*. 2020;10:11996.
76. Puddifoot CA, Wu M, Sung R-J, Joiner WJ. Ly6h regulates trafficking of $\alpha 7$ nicotinic acetylcholine receptors and nicotine-induced potentiation of glutamatergic signaling. *J Neurosci*. 2015;35:3420–30.
77. Brennaman LH, Zhang X, Guan H, Triplett JW, Brown A, Demyanenko GP, et al. Polysialylated NCAM and EphrinA/EphA regulate synaptic development of GABAergic interneurons in prefrontal cortex. *Cereb Cortex*. 2013;23:162–77.
78. Chen HC, Loh HH. μ -Opioid receptor gene expression: the role of NCAM. *Neuroscience* 2001;108:7–15.
79. Duncan BW, Murphy KE, Maness PF. Molecular mechanisms of L1 and NCAM adhesion molecules in synaptic pruning, plasticity, and stabilization. *Front Cell Dev Biol*. 2021;9:625340.
80. Nelson EC, Lynskey MT, Heath AC, Wray N, Agrawal A, Shand FL, et al. ANKK1, TTC12, and NCAM1 polymorphisms and heroin dependence—importance of considering drug exposure. *JAMA Psychiatry*. 2013;70:325–33.
81. Polo-Parada L, Bose CM, Plattner F, Landmesser LT. Distinct roles of different neural cell adhesion molecule (NCAM) isoforms in synaptic maturation revealed by analysis of NCAM 180 kDa isoform-deficient mice. *J Neurosci*. 2004;24:1852–64.
82. Bae Y-S, Chung W, Han K, Park KY, Kim H, Kim E, et al. Down-regulation of RalBP1 expression reduces seizure threshold and synaptic inhibition in mice. *Biochem Biophys Res Commun*. 2013;433:175–80.
83. Chen M-S, Kim H, Jagot-Lacoussiere L, Maurel P. Cdm3 (Nec1-1) interferes with the activation of the PI3 kinase/Akt signaling cascade and inhibits Schwann cell myelination in vitro. *Glia*. 2016;64:2247–62.
84. Kamimura K, Maeda N. Glypicans and heparan sulfate in synaptic development, neural plasticity, and neurological disorders. *Front Neural Circuits*. 2021;15:595596.
85. Beurrier C, Faideau M, Bennouar K-E, Escartin C, Kerkerian-Le Goff L, Bonvento G, et al. Ciliary neurotrophic factor protects striatal neurons against excitotoxicity by enhancing glial glutamate uptake. *PLoS ONE*. 2010;5:e8550.
86. Wang Q, Chiu S-L, Koropouli E, Hong I, Mitchell S, Easwaran TP, et al. Neuropilin-2/PlexinA3 receptors associate with GluA1 and mediate Semaphorin-3F-dependent homeostatic scaling in cortical neurons. *Neuron*. 2017;96:1084–98.e7.
87. Yamashita N, Usui H, Nakamura F, Chen S, Sasaki Y, Hida T, et al. Plexin-A4-dependent retrograde semaphorin 3A signalling regulates the dendritic localization of GluA2-containing AMPA receptors. *Nat Commun*. 2014;5:3424.
88. Awasthi A, Ramachandran B, Ahmed S, Benito E, Shinoda Y, Nitzan N, et al. Synaptotagmin-3 drives AMPA receptor endocytosis, depression of synapse strength, and forgetting. *Science*. 2019;363:eaav1483.
89. Jin X-T, Galvan A, Wichmann T, Smith Y. Localization and function of GABA transporters GAT-1 and GAT-3 in the basal ganglia. *Front Syst Neurosci*. 2011;5:63.
90. Savtchenko L, Megalogeni M, Rusakov DA, Walker MC, Pavlov I. Synaptic GABA release prevents GABA transporter type-1 reversal during excessive network activity. *Nat Commun*. 2015;6:6597.
91. Yuan A, Rao MV, Veeranna, Nixon RA. Neurofilaments at a glance. *J Cell Sci*. 2012;125:3257–63.
92. Nikoshkov A, Drakenberg K, Wang X, Horvath MCS, Keller E, Hurd YL. Opioid neuropeptide genotypes in relation to heroin abuse: Dopamine tone contributes to reversed mesolimbic proenkephalin expression. *Proc Natl Acad Sci USA*. 2008;105:786–91.
93. Kieffer BL, Gav eriaux-Ruff C. Exploring the opioid system by gene knockout. *Prog Neurobiol*. 2002;66:285–306.
94. Chaplot K, Jarvela TS, Lindberg I. Secreted chaperones in neurodegeneration. *Front Aging Neurosci*. 2020;12:268.
95. Ram A, Edwards T, McCarty A, Afrose L, McDermott MV, Bobeck EN. GPR171 agonist reduces chronic neuropathic and inflammatory pain in male, but not female mice. *Front Pain Res*. 2021;2:695396.
96. Castrogiovanni P, Sanfilippo C, Imbesi R, Maugeri G, Lo Furno D, Tibullo D, et al. Brain CHID1 expression correlates with NRGN and CALB1 in healthy subjects and AD patients. *Cells*. 2021;10:882.
97. Manavalan A, Mishra M, Feng L, Sze SK, Akatsu H, Heese K. Brain site-specific proteome changes in aging-related dementia. *Exp Mol Med*. 2013;45:e39–e39.
98. Chanaday NL, Kavalali ET. Role of the endoplasmic reticulum in synaptic transmission. *Curr Opin Neurobiol*. 2022;73:102538.
99. Lewis JE, Brameld JM, Jethwa PH. Neuroendocrine role for VGF. *Front Endocrinol*. 2015;6:3.
100. Rombaut B, Kessels S, Schepers M, Tiane A, Paes D, Solomina Y, et al. PDE inhibition in distinct cell types to reclaim the balance of synaptic plasticity. *Theranostics*. 2021;11:2080–97.
101. Sil S, Periyasamy P, Thangaraj A, Chivero ET, Buch S. PDGF/PDGFR axis in the neural systems. *Mol Asp Med*. 2018;62:63–74.
102. Puig S, Barker KE, Szott SR, Kann PT, Morris JS, Gutstein HB. Spinal opioid tolerance depends upon platelet-derived growth factor receptor- β signaling, not μ -opioid receptor internalization. *Mol Pharmacol*. 2020;98:487–96.
103. Wang Y, Barker K, Shi S, Diaz M, Mo B, Gutstein HB. Blockade of PDGFR- β activation eliminates morphine analgesic tolerance. *Nat Med*. 2012;18:385–7.
104. Zhou Z, Meng Y, Asrar S, Todorovski Z, Jia Z. A critical role of Rho-kinase ROCK2 in the regulation of spine and synaptic function. *Neuropharmacology*. 2009;56:81–9.
105. Strawbridge RJ, Ward J, Lyall LM, Tunbridge EM, Cullen B, Graham N, et al. Genetics of self-reported risk-taking behaviour, trans-ethnic consistency and relevance to brain gene expression. *Transl Psychiatry*. 2018;8:1–11.
106. Jeanne M, Demory H, Moutal A, Vuillaume M-L, Blesson S, Th epault R-A, et al. Missense variants in DPY5L5 cause a neurodevelopmental disorder with corpus callosum agenesis and cerebellar abnormalities. *Am J Hum Genet*. 2021;108:951–61.
107. Gawden-Bone CM, Frazer GL, Richard AC, Ma CY, Strega K, Griffiths GM. PIP5 kinases regulate membrane phosphoinositide and actin composition for targeted granule secretion by cytotoxic lymphocytes. *Immunity*. 2018;49:427–37.e4.

108. Schaffer TB, Smith JE, Cook EK, Phan T, Margolis SS. PKC ϵ inhibits neuronal dendritic spine development through dual phosphorylation of Ephexin5. *Cell Rep.* 2018;25:2470–83.e8.
109. Russell SE, Puttick DJ, Sawyer AM, Potter DN, Mague S, Carlezon WA, et al. Nucleus accumbens AMPA receptors are necessary for morphine-withdrawal-induced negative-affective states in rats. *J Neurosci.* 2016;36:5748–62.
110. Hearing M, Graziane N, Dong Y, Thomas MJ. Opioid and psychostimulant plasticity: targeting overlap in nucleus accumbens glutamate signaling. *Trends Pharmacol Sci.* 2018;39:276–94.
111. Mallard TT, Ashenhurst JR, Harden KP, Fromme K. GABRA2, alcohol, and illicit drug use: an event-level model of genetic risk for polysubstance use. *J Abnorm Psychol.* 2018;127:190–201.
112. Enoch M-A, Hodgkinson CA, Yuan Q, Shen P-H, Goldman D, Roy A. The influence of GABRA2, childhood trauma, and their interaction on alcohol, heroin, and cocaine dependence. *Biol Psychiatry.* 2010;67:20–7.
113. Sun Y, Zhang Y, Zhang D, Chang S, Jing R, Yue W, et al. GABRA2 rs279858-linked variants are associated with disrupted structural connectome of reward circuits in heroin abusers. *Transl Psychiatry.* 2018;8:1–10.
114. Nirwane A, Yao Y. Laminins and their receptors in the CNS. *Biol Rev Camb Philos Soc.* 2019;94:283–306.
115. Gómez-López S, Martínez-Silva AV, Montiel T, Osorio-Gómez D, Bermúdez-Rattoni F, Massieu L, et al. Neural ablation of the PARK10 candidate Plpp3 leads to dopaminergic transmission deficits without neurodegeneration. *Sci Rep.* 2016;6:24028.
116. Zhang S, Glukhova SA, Caldwell KA, Caldwell GA. NCEH-1 modulates cholesterol metabolism and protects against α -synuclein toxicity in a *C. elegans* model of Parkinson's disease. *Hum Mol Genet.* 2017;26:3823–36.
117. Jin J, Yu Q, Han C, Hu X, Xu S, Wang Q, et al. LRRFIP2 negatively regulates NLRP3 inflammasome activation in macrophages by promoting Flightless-I-mediated caspase-1 inhibition. *Nat Commun.* 2013;4:2075.
118. Wright BD, Loo L, Street SE, Ma A, Taylor-Blake B, Stashko MA, et al. The lipid kinase PIP5K1C regulates pain signaling and sensitization. *Neuron.* 2014;82:836–47.
119. Pavelitz T, Gray LT, Padilla SL, Bailey AD, Weiner AM. PGBD5: a neural-specific intron-containing piggyBac transposase domesticated over 500 million years ago and conserved from cephalochordates to humans. *Mob DNA.* 2013;4:23.
120. Cai Z, Ratka A. Opioid system and Alzheimer's disease. *Neuromol Med.* 2012;14:91–111.
121. Kennedy GJ. Bad news and good: opioids are associated with the incidence of dementia, but the effect is substantial only for those 75–80 years of age. *Am J Geriatr Psychiatry.* 2023;31:324–5.
122. Anthony IC, Norrby KE, Dingwall T, Carnie FW, Millar T, Arango JC, et al. Predisposition to accelerated Alzheimer-related changes in the brains of human immunodeficiency virus negative opiate abusers. *Brain J Neurol.* 2010;133:3685–98.
123. Mao L, Wang K, Zhang P, Ren S, Sun J, Yang M, et al. Carbonyl reductase 1 attenuates ischemic brain injury by reducing oxidative stress and neuroinflammation. *Transl Stroke Res.* 2021;12:711–24.
124. De Rossi P, Nomura T, Andrew RJ, Masse NY, Sampathkumar V, Musial TF, et al. Neuronal BIN1 regulates presynaptic neurotransmitter release and memory consolidation. *Cell Rep.* 2020;30:3520–35.e7.
125. Ye H, Ojelade SA, Li-Kroeger D, Zuo Z, Wang L, Li Y, et al. Retromer subunit, VPS29, regulates synaptic transmission and is required for endolysosomal function in the aging brain. *Elife.* 2020;9:e51977.
126. Chen X, Lu W, Wu D. Sirtuin 2 (SIRT2): confusing roles in the pathophysiology of neurological disorders. *Front Neurosci.* 2021;15:614107.
127. Ferguson D, Koo JW, Feng J, Heller E, Rabkin J, Heshmati M, et al. Essential role of SIRT1 signaling in the nucleus accumbens in cocaine and morphine action. *J Neurosci.* 2013;33:16088–98.
128. Zhao B, Zhu Y, Wang W, Cui H, Wang Y, Lai J. Analysis of variations in the glutamate receptor, N-methyl D-aspartate 2A (GRIN2A) gene reveals their relative importance as genetic susceptibility factors for heroin addiction. *PLoS ONE.* 2013;8:e70817.
129. Elmasri M, Lotti JS, Aziz W, Steele OG, Karachaliou E, Sakimura K, et al. Synaptic dysfunction by mutations in GRIN2B: influence of triheteromeric NMDA receptors on gain-of-function and loss-of-function mutant classification. *Brain Sci.* 2022;12:789.
130. Sheng Z, Liu Q, Cheng C, Li M, Barash J, Kofke WA, et al. Fentanyl induces autism-like behaviours in mice by hypermethylation of the glutamate receptor gene *Grin2b*. *Br J Anaesth.* 2022;129:544–54.
131. Lee E, Lee S, Shin JJ, Choi W, Chung C, Lee S, et al. Excitatory synapses and gap junctions cooperate to improve Pv neuronal burst firing and cortical social cognition in Shank2-mutant mice. *Nat Commun.* 2021;12:5116.
132. Bryant DT, Landles C, Papadopoulou AS, Benjamin AC, Duckworth JK, Rosahl T, et al. Disruption to schizophrenia-associated gene *Fez1* in the hippocampus of HDAC11 knockout mice. *Sci Rep.* 2017;7:11900.
133. Glausier JR, Kimoto S, Fish KN, Lewis DA. Lower glutamic acid decarboxylase 65-kDa isoform messenger RNA and protein levels in the prefrontal cortex in schizoaffective disorder but not schizophrenia. *Biol Psychiatry.* 2015;77:167–76.
134. Kowalski EA, Chen J, Hazy A, Fritsch LE, Gudenschwager-Basso EK, Chen M, et al. Peripheral loss of EphA4 ameliorates TBI-induced neuroinflammation and tissue damage. *J Neuroinflammation.* 2019;16:210.
135. Bott CJ, Winckler B. Intermediate filaments in developing neurons: beyond structure. *Cytoskeleton* 2020;77:110–28.
136. Borgkvist A, Usiello A, Greengard P, Fisone G. Activation of the cAMP/PKA/DARPP-32 signaling pathway is required for morphine psychomotor stimulation but not for morphine reward. *Neuropsychopharmacology.* 2007;32:1995–2003.
137. Gould TD, Manji HK. DARPP-32: a molecular switch at the nexus of reward pathway plasticity. *Proc Natl Acad Sci USA.* 2005;102:253–4.
138. Mahajan SD, Aalinkeel R, Reynolds JL, Nair BB, Sykes DE, Hu Z, et al. Therapeutic targeting of 'DARPP-32': a key signaling molecule in the dopaminergic pathway for the treatment of opiate addiction. *Int Rev Neurobiol.* 2009;88:199–222.
139. Brami-Cherrier K, Lewis RG, Cervantes M, Liu Y, Tognini P, Baldi P, et al. Cocaine-mediated circadian reprogramming in the striatum through dopamine D2R and PPAR α activation. *Nat Commun.* 2020;11:4448.
140. Bumgarner JR, McCray EW, Nelson RJ. The disruptive relationship among circadian rhythms, pain, and opioids. *Front Neurosci.* 2023;17:1109480.
141. Gallerani M, Manfredini R, Dal Monte D, Calò G, Brunaldi V, Simonato M. Circadian differences in the individual sensitivity to opiate overdose. *Crit Care Med.* 2001;29:96–101.
142. Ke Y, Weng M, Chhetri G, Usman M, Li Y, Yu Q, et al. Trappc9 deficiency in mice impairs learning and memory by causing imbalance of dopamine D1 and D2 neurons. *Sci Adv.* 2020;6:eabb7781.
143. Carter SD, Hampton CM, Langlois R, Melero R, Farino ZJ, Calderon MJ, et al. Ribosome-associated vesicles: A dynamic subcompartment of the endoplasmic reticulum in secretory cells. *Sci Adv.* 2020;6:eaay9572.
144. Mauvoisin D, Wang J, Jouffe C, Martin E, Atger F, Waridel P, et al. Circadian clock-dependent and -independent rhythmic proteomes implement distinct diurnal functions in mouse liver. *Proc Natl Acad Sci USA.* 2014;111:167–72.
145. Ancona Esselmann SG, Diaz-Alonso J, Levy JM, Bemben MA, Nicoll RA. Synaptic homeostasis requires the membrane-proximal carboxy tail of GluA2. *Proc Natl Acad Sci USA.* 2017;114:13266–71.
146. Weinhard L, di Bartolomei G, Bolasco G, Machado P, Schieber NL, Neniskyte U, et al. Microglia remodel synapses by presynaptic trogocytosis and spine head filopodia induction. *Nat Commun.* 2018;9:1228.
147. Calcia MA, Bonsall DR, Bloomfield PS, Selvaraj S, Barichello T, Howes OD. Stress and neuroinflammation: a systematic review of the effects of stress on microglia and the implications for mental illness. *Psychopharmacology.* 2016;233:1637–50.
148. Gamble MC, Williams BR, Singh N, Posa L, Freyberg Z, Logan RW, et al. Mu-opioid receptor and receptor tyrosine kinase crosstalk: Implications in mechanisms of opioid tolerance, reduced analgesia to neuropathic pain, dependence, and reward. *Front Syst Neurosci.* 2022;16:1059089.
149. Lee U, Choi C, Ryu SH, Park D, Lee S-E, Kim K, et al. SCAMP5 plays a critical role in axonal trafficking and synaptic localization of NHE6 to adjust quantal size at glutamatergic synapses. *Proc Natl Acad Sci USA.* 2021;118:e2011371118.

ACKNOWLEDGEMENTS

Thank you to the staff and technicians who work diligently as part of the Brain Tissue Donation Program at the University of Pittsburgh. Postmortem human brain tissue was provided by the University of Pittsburgh Brain Tissue Donation Program and the National Institutes of Health NeuroBioBank at the University of Pittsburgh.

AUTHOR CONTRIBUTIONS

MLS and RWL obtained funding for the project. JRG, DAL, MLS, MLM, and RWL designed and coordinated the study. SP, RS, MAS, MAH, SMK, JRG, and MLM processed samples for proteomics. SP, XX, ZF, GCT, AY, MLM, and RWL conducted analyses and data interpretation. SP, XX, MLS, MLM, and RWL wrote the manuscript. All authors read and approved the final version of the manuscript.

FUNDING

The research reported in this article was supported by: Hamilton Family Prize for Basic Neuroscience Research in Psychiatry at the University of Pittsburgh School of Medicine (RWL); National Heart, Lung, and Blood Institute (R01HL150432, RWL); and National Institute on Drug Abuse (R01DA051390, MLS and RWL).

COMPETING INTERESTS

The authors report no competing interests.

ADDITIONAL INFORMATION

Supplementary information The online version contains supplementary material available at <https://doi.org/10.1038/s41380-023-02241-6>.

Correspondence and requests for materials should be addressed to Matthew L. MacDonald or Ryan W. Logan.

Reprints and permission information is available at <http://www.nature.com/reprints>

Publisher's note Springer Nature remains neutral with regard to jurisdictional claims in published maps and institutional affiliations.



Open Access This article is licensed under a Creative Commons Attribution 4.0 International License, which permits use, sharing, adaptation, distribution and reproduction in any medium or format, as long as you give appropriate credit to the original author(s) and the source, provide a link to the Creative Commons licence, and indicate if changes were made. The images or other third party material in this article are included in the article's Creative Commons licence, unless indicated otherwise in a credit line to the material. If material is not included in the article's Creative Commons licence and your intended use is not permitted by statutory regulation or exceeds the permitted use, you will need to obtain permission directly from the copyright holder. To view a copy of this licence, visit <http://creativecommons.org/licenses/by/4.0/>.

© The Author(s) 2023